The role of histone lysine demethylase 2B in the pathology of canine hemangiosarcoma
(イヌ血管肉腫の病態におけるヒストンリジン脱メチル化酵素 2B の役割に関する研究)

Kevin Christian Montecillo Gulay
Laboratory of Comparative Pathology
Department of Clinical Sciences
Graduate School of Veterinary Medicine
Hokkaido University

Contents

Abbreviations

ATR: Ataxia Telangiectasia And Rad3-Related Protein

BAX: BCL2 Associated X

BRCA2: Breast Cancer Type 2 Susceptibility Protein

CCR7: C-C Motif Chemokine Receptor 7

CD40: Cluster of differentiation 40

CDC25A: Cell Division Cycle 25A

COL1A2: Collagen Type I Alpha 2 Chain

DLL1: Delta Like Canonical Notch Ligand 1

DOT1L: DOT1 Like Histone Lysine Methyltransferase

E2F1: E2F Transcription Factor 1

EZH1: Enhancer Of Zeste Homolog 1

EZH2: Enhancer Of Zeste Homolog 2

FGFR1: Fibroblast Growth Factor Receptor 1

FGFR2: Fibroblast Growth Factor Receptor 2

G9A: Euchromatic Histone Lysine Methyltransferase 2

HEY1: Hes Related Family BHLH Transcription Factor With YRPW Motif 1

HEY2: Hes Related Family BHLH Transcription Factor With YRPW Motif 2

HSPA5: Heat Shock Protein Family A (Hsp70) Member 5

HSPA8: Heat Shock Protein Family A (Hsp70) Member 8

IF144L: Interferon Induced Protein 44 Like

INSIG1: Insulin Induced Gene 1

ITGB3: Integrin Beta-3

JAG1: Jagged Canonical Notch Ligand 1

JAG2: Jagged Canonical Notch Ligand 2

JAK1: Janus Kinase 1

JAK2: Janus Kinase 2

KDM1A: Lysine Demethylase 1A

KDM2A: Lysine Demethylase 2A

KDM2B: Lysine Demethylase 2B

KDM3A: Lysine Demethylase 3A

KDM4A: Lysine Demethylase 4A

KDM4B: Lysine Demethylase 4B

KDM4C: Lysine Demethylase 4C

KDM5A: Lysine Demethylase 5A

KDM5B: Lysine Demethylase 5B

KDM6A: Lysine Demethylase 6A

KDM6B: Lysine Demethylase 6B

KDM7A: Lysine Demethylase 7A

MCL1: Myeloid Cell Leukemia Sequence 1

MLL1: Mixed Lineage Leukemia 1

MLL3: Mixed Lineage Leukemia 3

MYC: Proto-Oncogene C-Myc

NOCTH2: Neurogenic Locus Notch Homolog Protein 2

NOTCH1: Neurogenic Locus Notch Homolog Protein 1

NSD1: Nuclear Receptor Binding SET Domain Protein 1

OAS1: 2'-5'-Oligoadenylate Synthetase 1

OAS2: 2'-5'-Oligoadenylate Synthetase 2

$P15^{INK4B}$: Cyclin Dependent Kinase Inhibitor 2B

$P16^{INK4A}$: Cyclin Dependent Kinase Inhibitor 2A

p18: Cyclin Dependent Kinase Inhibitor 2C

PDK3: Pyruvate Dehydrogenase Kinase 3

PLOD2: Procollagen-Lysine,2-Oxoglutarate 5-Dioxygenase 2

PPARG: Peroxisome Proliferator Activated Receptor Gamma

PROCR: Protein C Receptor

RB1: Retinoblastoma 1

SDC1: Syndecan 1

SET: SET Nuclear Proto-Oncogene

SETD2: SET Domain Containing 2

SETD4: SET Domain Containing 4

SETD5: SET Domain Containing 5

SETD6: SET Domain Containing 6

SETD7: SET Domain Containing 7

SETD9: SET Domain Containing 9

SETMAR: SET Domain And Mariner Transposase Fusion Gene

SMYD3: SET And MYND Domain Containing 3

SMYD4: SET And MYND Domain Containing 4

SMYD5: SET And MYND Domain Containing 5

SUV39H1: Suppressor Of Variegation 3-9 Homolog 1

SUV39H2: Suppressor Of Variegation 3-9 Homolog 2

TBP: TATA-Box Binding Protein

TGFBR3: Transforming Growth Factor Beta Receptor 3

TNFAIP3: TNF Alpha Induced Protein 3

VEGFA: Vascular Endothelial Growth Factor A

VLDLR: Very-Low-Density-Lipoprotein Receptor

Notes

The contents of this thesis were published in the journal article below.

List of published articles

1. Gulay KCM, Aoshima K, Shibata Y, Yasui H, Yan Q, Kobayashi A, Kimura T. KDM2B promotes cell viability by enhancing DNA damage response in canine hemangiosarcoma. J Genet Genomics. 2021 Mar 10:S1673-8527(21)00044-8. doi: 10.1016/j.jgg.2021.02.005. Epub ahead of print.

Preface

Chemotherapy, surgery, and radiotherapy are among the most commonly used cancer treatment(Arruebo et al., 2011). Chemotherapy began in the 1930s and was first used to treat lymphoma and leukemia(Goodman & Wintrobe, 1946). Most common drugs used in chemotherapy are 5-fluorouracil and doxorubicin which were first used in the 1950s and 1980s, respectively(Heidelberger et al., 1957). These decades-old drugs are still being used to date to treat malignancies in humans and animals despite the numerous adverse effects associated with them. Surgery, on the other hand, is effective for non-metastatic and non-invasive tumors but cannot do much once the tumor has spread to other parts of the body (Adjiri, 2016). Radiotherapy is one of the most common cancer treatment modalities because it provides excellent tumor control while preserving normal tissues and causing less systemic side effects. However, radiation-treated tumors can sometimes recur with radio-resistance which results to treatment failure (J. J. Kim & Tannock, 2005). Moreover, radiation has been shown to induce genetic instability and chromosomal rearrangements which can lead to the development of a secondary tumor (Huang et al., 2003). Intriguingly, studies showed that sub-lethal doses of radiation can sometimes promote cancer metastasis by inducing migration potential and invasiveness (Wild-Bode et al., 2001). It is very clear that alternative treatments for cancer are needed.

Hemangiosarcoma (HSA), a vascular tumor, is the most common splenic neoplasm in dogs where it usually occurs between 6 to 17 years of age (Prymak et al., 1988). Middle to large breeds is most commonly afflicted with HSA. A sex predilection has not been established but neutering may have an effect in its incidence(Prymak et al., 1988). Any tissue or organ with vascular structures may develop HSA. The spleen, right atrium of the heart, liver, subcutis, and dermis are the most common sites for HSA tumor development (Yamamoto et al., 2013). HSA also occurs infrequently in cats, horses, mice, and humans (Johannes et al., 2007; Sastry, 1951; Shimizu et al., 1974; Young et al., 2010). Little is known about the genes which are responsible for the induction, maintenance, and progression of HSA. Future research in HSA should be directed in finding the genes responsible for its pathology.

Epigenetics is characterized as heritable variations in gene expression that are

not caused by changes in DNA sequence (Dawson & Kouzarides, 2012). DNA methylation, chromatin structure changes, imprinting loss, and non-coding RNA are the most common epigenetic mechanisms. Numerous studies on the epigenome and cancer supported the epigenetic contribution to cancer development. For example, recurrent mutations of the histone methyltransferase *MLL2* are found in nearly 90 percent of cases of follicular lymphoma(Morin et al., 2011). *UTX*, a histone demethylase, has been shown to be mutated in up to 12 histologically distinct cancers(van Haaften et al., 2009). The most commonly affected epigenetic pathways are histone acetylation and methylation, according to a compilation of epigenetic regulators mutated in cancer(Dawson & Kouzarides, 2012). Unfortunately, epigenetic studies in HSA are non-existent up to present.

This thesis was dedicated to find the oncogenes responsible for the pathology of HSA by studying the importance and role of epigenetics in HSA. In addition, this thesis also aimed to find a potential therapeutic alternative to the decades-old chemotherapeutic methods that we deploy to treat HSA. Moreover, the author also sought to shed some light towards understanding the role of the tumor microenvironment and the immune responses in HSA pathology to pave the way for future HSA research.

Introduction

Canine hemangiosarcoma (HSA) is a highly malignant tumor of vascular endothelial cells. It is an aggressive tumor with high rates of local recurrence and metastasis, and a low overall survival time (J.-H. Kim et al., 2015). Its high cellular heterogeneity has limited genomic and pathogenesis studies in HSA. Genomic analyses have revealed that HSA cells have somatic coding mutations in the *TP53*, *PIK3CA*, and *PIK3R1*. Furthermore, *CDKN2A/B* were found to be consistently deleted and copies of *VEGFA*, *KDR* and *KIT* were gained (Megquier et al., 2019). The oncogene involved in HSA, however, is still unknown.

Epigenetic mechanisms are essential for reproduction, embryonic development, and maintenance of normal cell function in eukaryotes(Sharma et al., 2010). Generally, the genetic alterations that cause tumorigenesis are combined with epigenetic shifts, such as aberrant DNA methylation and histone modifications, which may help oncogenic drivers improve cancer development, metastasis, and resistance to therapies (Moosavi & Motevalizadeh Ardekani, 2016). Histone lysine demethylase 2B (KDM2B; also known as NDY1 and FBXL10), an H3K4me3, H3K36me2/3 and H3K79me3 demethylase, acts as a tumor suppressor in gastric cancer by downregulating glycolysis, and tumor-derived mutation in KDM2B enhances cell proliferation through the inability of c-FOS degradation (Hong et al., 2016). Alternatively, KDM2B can also act as an oncogene in various types of cancers. In leukemia, KDM2B is highly expressed and is sufficient to transform hematopoietic progenitor cells (He et al., 2011). In breast cancer, KDM2B regulates polycomb complexes and controls self-renewal of breast cancer stem cells (Kottakis et al., 2014). This bifunctional activity means that the role of KDM2B in tumors is highly context dependent and must be evaluated carefully (Yan et al., 2018a). While epigenetics is highly involved in pathogenesis of many cancers, its role in HSA is still unknown.

Treatment of HSA is carried out by tumor excision and chemotherapy mainly with doxorubicin (Clifford et al., 2000). The mean survival time for surgical treatment is 3 months while the mean survival time for surgical treatment with chemotherapy is less than a year (Batschinski et al., 2018). Chemotherapeutic drugs fail to improve survival times of cancer patients due to the non-specificity of their cytotoxic effects in the

cardiomyocytes, brain, liver and intestine (Carvalho et al., 2009; Odom et al., 1992). A more effective, specific, and safer treatment for HSA is warranted.

Histone demethylase inhibitors are effective agents for anticancer treatment. In a previous study, GSK-J4, a histone demethylase inhibitor, decreased AML disease progression by downregulating DNA replication and cell cycle-related pathways through the enrichment of H3K27me3 (Y. Li et al., 2018). GSK-J4 was initially developed as a KDM6 inhibitor, but it was found to inhibit the catalytic activity of a wide range of JmjC domain-containing histone demethylases including KDM2B (Heinemann et al., 2014). Epigenetic therapy may provide additional treatment option, but no epigenetic drug has tested for HSA.

In this study, I sought to establish the pathogenesis and to find a therapeutic alternative for HSA by examining the role of epigenetic regulators.

Materials and methods

Cell culture

The HSA cell lines were donated by Dr. Sakai (Gifu University) (Murai et al., 2012) and cultured as described previously(Aoshima et al., 2018). Canine aortic endothelial cells (CnAOEC) were purchased from Cell Applications (CA, USA). CnAOEC was cultured in Endothelial Cell Growth Medium 2 Kit (Takara Bio, Inc. Kusatsu, Japan). All cells used were routinely tested for *Mycoplasma* using PCR and were submitted to ICLAS Monitoring Center (Kawasaki, Japan) for Mouse hepatitis virus testing (R. Harasawa et al., 1993; Ryô Harasawa et al., 2005).

Mice

All mouse experiments were performed under the AAALAC guidelines in Yale University (protocol number: 2018-11286) and Hokkaido University (protocol number:19-0130). All animal experiments comply with the ARRIVE guidelines and the National Institutes of Health guide for the care and use of Laboratory animals. Seven-week-old female Balb/c Nude mice purchased from Charles River Laboratories (MA,

USA) were used for *KDM2B* knockdown experiments. Six-week-old female KSN/Slc mice purchased from Japan SLC, Inc. (Shizuoka, Japan) were used for drug treatment experiments. Mice were kept in a temperature-controlled specific-pathogen-free facility on a 12 hr light/dark cycle. Animals in all experimental groups were examined at least twice weekly for tumorigenesis.

Tumor xenograft studies

A day before tumor inoculation, KSN/Slc mice were treated with 100 μL of 2.5 mg/mL anti-asialo GM1 (Fujifilm Wako Pure Chemical Industries, Osaka, Japan) to increase the success rate of transplantation by depleting NK cells (Yoshino et al., 2000). JuB2 parental HSA cells and JuB2 cells expressing the shRNAs or the scramble shRNA for *KDM2B* in the presence of doxycycline were cultured in 15 cm dishes without doxycycline. Mice were randomly assigned in each group. Three million HSA cells were resuspended in Corning® Matrigel® Basement Membrane Matrix (Corning Inc. NY, USA) and inoculated subcutaneously in mice anesthetized with 3% isoflurane or 100 mg/kg Ketamine and 10 mg/kg Xylazine. Tumor sizes were measured twice weekly one week after inoculation. When the largest tumor reached 150 mm^3 in volume, mice were fed doxycycline-containing food to induce shRNA expression, or treated thrice weekly for three weeks with 50 mg/kg DMSO, 50 mg/kg GSK-J4 (Medchemexpress, NJ, USA), or 5 mg/kg doxorubicin (Fujifilm Wako Pure Chemical Industries) intraperitoneally. Mice were euthanized with CO_2 when tumors reached 500 mm^3 in volume or when mice exhibited abnormal behavior. Tumors and major organs were weighed and fixed in 10% neutral buffered formalin for histological examination.

Western Blotting

SDS lysis buffer (2% SDS, 50 mM Tris-HCl (pH6.8), 1mM EDTA (pH 8.0)) with EDTA-free proteinase inhibitor cocktail (Sigma-Aldrich, MO, USA) was added in cultured cells. Cell lysates were then sonicated using BRANSON Sonifier 450 (Branson Ultrasonics Corporation, CT, USA) for two secs. Protein concentrations were measured with the Pierce™ BCA Protein Assay Kit (Thermo Fisher Scientific) before adding 4X Sample loading buffer (200 mM Tris-HCl buffer (pH 6.8), 8% SDS, 40% Glycerol, 1% bromophenol blue, 20% 2-mercaptoethanol) and denaturing at 98°C for 10 mins. 3 μg

proteins were separated by SDS-PAGE and electrotransferred onto Immobilon®-P transfer membranes (Merck Millipore, MA, USA), blocked with 5% skim milk in Tris-buffered saline with 5% Tween 20 (TBST), or 5% BSA in TBST for 1 hour at room temperature (RT) and incubated with primary antibody in Can Get Signal Solution® 1 (TOYOBO, Osaka, Japan) overnight at 4°C. The membranes were washed with TBST three times before incubating with the corresponding secondary anti-mouse or anti-rabbit IgG antibody (GE Healthcare) in Can Get Signal Solution® 2 (TOYOBO). Signals were developed with Immobilon® Western Chemiluminescent HRP substrate (Merck Millipore) and visualized in ImageQuant LAS 4000 mini luminescent image analyzer (GE Healthcare). Captured data were processed using ImageJ software (Schneider et al., 2012). The list of antibodies used in this study can be found as Table 1.

Quantitative RT-PCR (qRT-PCR)

Total RNA was extracted with Nucleospin® RNA isolation kit (Macherey-Nagel GmbH & Co. Düren, Germany) following the manufacturer's instructions. Synthesis of cDNA was performed using the PrimeScript™ Reverse Transcriptase (Takara Bio, Inc.) according to the manufacturer's instructions. qRT-PCR was performed with StepOne™ Real Time System (Thermo Fisher Scientific). The oligos for qRT-PCR were designed as described elsewhere (Aoshima et al., 2018; Peters et al., 2007), and listed within Table 2.

RNA-sequencing

CnAOEC or JuB2 HSA cells were cultured in 10 cm dishes in triplicate. Upon reaching 80% confluency, RNA was extracted with Nucleospin® RNA isolation kit (Macherey-Nagel GmbH & Co.) following the manufacturer's instructions. RNA samples were submitted to Annoroad (Beijing, China) for further analyses. Quality testing was carried by measuring RNA integrity (RIN), $OD_{260/280}$ and $OD_{260/230}$. All samples had an RIN of 9.3 or better and OD readings were within the range of 1.8-2.2. RNA-seq libraries were constructed using NEBNext® Ultra RNA Library Prep Kit for Ilumina® (New England Biolabs, MA, USA) and sequenced with the Illumina HiSeq X-Ten platform (Illumina, CA, USA) to generate a minimum of 20 million paired-end 150 bp reads. Sequencing reads were mapped to the canine reference genome CanFam3.1

using STAR and aligned using RSEM(Dobin et al., 2013; B. Li & Dewey, 2011). Differential expression analyses were carried out using edgeR(Robinson et al., 2010), and gene expression profiles were analyzed by GSEA v4.03(Mootha et al., 2003; Subramanian et al., 2005). The gene set database of h. all. v7.1. symbols. gmt (Hallmarks) was used.

shRNA vector construction

The shRNAs used in this study were designed using the Hannon lab shRNA design tool (http://hannonlab.cshl.edu/GH_shRNA.html, Cold Spring Harbor Laboratory). Oligos were inserted to pLKO.1-TRC or pInducer10-mir-RUP-PheS vector, a gift from David Root (Addgene plasmid # 10878; http://n2t.net/addgene:10878; RRID:Addgene_10878) (Moffat et al., 2006) and from Stephen Elledge (Addgene plasmid # 44011; http://n2t.net/addgene:44011; RRID:Addgene 44011) (Meerbrey et al., 2011), respectively. shRNA expressions were induced by supplementing 2 μM doxycycline in the culture medium. The list of oligonucleotide sequences used for shRNA knockdown can be found as Table 3.

Overexpression vector construction

The coding sequence of canine *KDM2B* (ENSCAFT00000093772.1) was cloned from cDNA synthesized from canine heart. Mutant KDM2B (H283Y, C586A, ΔPHD) were synthesized as described elsewhere (Edelheit et al., 2009). The amplicon tagged with FLAG sequences at its 3' end was ligated into CSII-CMV-MCS-IRES2-Bsd vector, a gift from Dr. Miyoshi (RIKEN BioResource Center, Ibaraki, Japan), with In-Fusion® HD Cloning Kit (Takara Bio, Inc.) according to the manufacturer's instruction. The list of oligonucleotide sequences used for CDS cloning are can be found as Table 4.

Lentivirus production

Lentiviruses were produced following a protocol described elsewhere with a slight modification that virus containing culture medium was used without concentration (Aoshima et al., 2018). Selection of positive clones were done by culturing of cells in 10 μg/ml blasticidin- or 4 μg/ml puromycin-containing cell medium.

Alkaline comet assay

JuB2 overexpressing shRNA for *KDM2B* or scrRNA were cultured in doxycycline-containing medium for four days. $4X10^4$ cells were used for alkaline comet assay as described previously[30]. 20 μg/mL propidium iodide (PI) was used for staining and the comets were visualized with BZ-9000 (BIOREVO) fluorescence microscope (Keyence, Osaka, Japan). Experiments were performed at least three times with triplicates.

Cell cycle analysis

When HSA cells reach 70% confluency, they were stained with 1 μL of 0.1M BrdU for 45 mins at 37°C. Cells were washed with phosphate-buffered saline (PBS) and trypsinized routinely. The cells were fixed in 70% ethanol overnight and washed with 0.5% Triton X-100 in PBS (PBST) before resuspending the cells in 500 μL of 2N HCl-0.5% Triton X-100 for 30 mins at RT and neutralizing with 500 μL of 0.1M $Na_2B_4O_7 \cdot 10H_2O$ (pH 8.5) for 30 mins at RT. After blocking with 1% BSA-0.3% Triton X-100 in PBS for 1 hr and washing with PBST, cells were counted and divided into two tubes; $2.5X10^5$ cells were used as controls and incubated in the blocking buffer while $6X10^5$ cells were incubated with anti-BrdU monoclonal antibody (1:100; MOBU-1 clone, B35128, Thermo Fisher Scientific) for 1 hr at RT. Excess primary antibodies were washed before staining with AlexaFluor 488 (1:1000; Thermo Fisher Scientific). DNA was stained with 10 μg/200 μL PI (Dojindo Molecular Technologies, Inc., Kumamoto, Japan). Cell cycle and cell proliferation were analyzed in BD FACSVerse™ flow cytometer (BD Biosciences, NJ, USA). Results were analyzed with FCS Express 4 software (De Novo Software, CA, USA). Experiments were performed at least three times with triplicates.

Cell viability analysis

Cell viability was measured with Cell Counting Kit-8 (Dojindo Molecular Technologies, Inc.) according to the manufacturer's instructions. The absorbance at 450 nm was measured with NanoDrop™ 2000 (Thermo Fisher Scientific). Determination of IC_{50} were performed using Ky Plot 6.0 software (KeyensLab, Inc.,

Tokyo, Japan) as described elsewhere (Morita et al., 2019). Experiments were performed at least three times with triplicates.

Colony formation assay

500 HSA cells were seeded in 6-well culture plates containing 2 mL normal medium supplemented with DMSO or 2 μM doxycycline. Cells were cultured until the largest colony reached 2 mm in diameter. Cells were fixed with 4% paraformaldehyde for 20 mins at RT, stained with 0.01% Crystal Violet (Sigma-Aldrich, MO, USA) for 30 mins at RT, and the images were captured with ChemiDoc XRS Plus (Bio-rad, CA, USA). Colony areas were measured using ColonyArea plugin for ImageJ (Guzmán et al., 2014; Schneider et al., 2012). Experiments were performed at least three times with triplicates.

Histopathology and immunohistochemistry (IHC)

Written informed consents were obtained from the owners of the patient dogs, and the samples were used only for research purposes. Hematoxylin and eosin staining was performed as described previously (Maharani et al., 2018). For IHC, tissue sections were deparaffinized, and heat-induced antigen retrieval was performed in citric acid buffer (pH 6.8) with a pressure cooker. Endogenous peroxidases were quenched with 0.3% H_2O_2 in methanol for 15 min at RT before blocking the tissue sections with 10% normal rabbit serum (Nichirei biosciences, Tokyo, Japan) for an hour at RT and incubating with KDM2B antibody (sc-293279, 1:50, Santa Cruz Biotechnology, CA, USA) overnight at 4°C. Slides were washed with 0.01M PBS before incubating with rabbit anti-mouse antibody (Nichirei biosciences) for 30 min at RT. Signals were developed with 3,3'-diaminobenzidine tetrahydrochloride (DAB; Dojindo).

Quantification of IHC scores

Histological slides were scanned with Nano Zoomer 2.0-RS (Hamamatsu Photonics, Hamamatsu, Japan) and processed in QuPath ver 0.2.1(Bankhead et al., 2017). Scanned slides were opened as Brightfield (H-DAB) in QuPath, and staining colors were automatically adjusted using Estimate Stain Vectors function. Healthy tumor regions or normal blood vessels were randomly selected, and cells were

detected using Cell Detection function. Cells were annotated based on their morphologies and location to allow QuPath to automatically classify each cell type correctly using the Create Detection Classifiers function. The measured data was exported and used for further analysis. We used Nuclear: DAB OD max scores for quantitative analysis because KDM2B signals were found only in heterochromatin regions in nuclei but they also had abundant euchromatin region. Furthermore, nonspecific signals from fibrin and erythrocytes were often misinterpreted as nuclear or cytoplasmic signals especially in normal endothelial cells, thus, to make the analysis as precise as possible, I decided to use max intensities in the nuclei.

Statistical analysis

Statistical analyses were performed with Microsoft Excel 2019 and R software (version 3.6.3). Student's *t*-test was used to analyze difference between two groups while the Tukey's test was used to analyze differences between multiple groups. The significance of the differences in tumor volumes of DMSO, GSK-J4 or doxorubicin-treated mice were compared using Dunnet's test while their survival post-treatment were compared using Log-rank test. *p*-values less than 0.05 were considered statistically significant.

Results

KDM2B is important for HSA cell survival

I first performed RNA-sequencing analysis of canine aortic endothelial cells (CnAOEC) and one HSA cell line, JuB2, to examine the expression levels of epigenetic modifiers. Among the differentially expressed genes, histone methyltransferases/demethylases, histone acetyltransferases/deacetylases, and DNA methyltransferase/demethylases were dysregulated in JuB2 compared with CnAOEC (Figs. 1A and 2A). Next, we performed qRT-PCR to verify RNA-seq results of histone methyltransferases/demethylases in CnAOEC and seven HSA cell lines. The result indicated that some histone methyltransferases/demethylases were highly upregulated in HSA cell lines at gene expression levels (Figs. 1B and 2B). While histone demethylases were relatively stable between HSA cells and CnAOEC compared with

histone methyltransferase, three histone demethylases (*KDM1A, KDM2A* and *KDM2B*) were markedly upregulated. I performed western blotting for KDM1A, KDM2A, and KDM2B and found that their protein levels were upregulated in all HSA cell lines compared with CnAOEC (Figs. 1C and 1D). These results suggest that epigenetic regulators are dysregulated in HSA and that histone demethylases KDM1A, KDM2A, and KDM2B are highly expressed in HSA.

To examine whether the overexpression of KDM1A, KDM2A and KDM2B have important functional roles in HSA, I designed three shRNA sequences for each gene to knockdown KDM1A, KDM2A and KDM2B. I also designed two scramble shRNAs (scrRNA) to serve as controls. These shRNAs were expressed in HSA cell lines using a doxycycline (Dox)-inducible vector system. Knockdown was verified with western blotting after four days of Dox treatment (Figs. 3A and 4A). Knockdown of KDM1A and KDM2A did not have short-term effects on JuB2 cell viability, whereas knockdown of KDM2B significantly decreased JuB2 cell viability within four days (Figs. 3B and 4B). To evaluate the long-term effects of KDM1A, KDM2A, and KDM2B silencing on JuB2 cell survival, I performed colony formation assay and found that KDM1A or KDM2A knockdown inhibited JuB2 colony formation, whereas KDM2B knockdown significantly reduced the number of colonies of JuB2 (Figs. 3C, 3D, 4C, 4D). KDM2B knockdown with constitutively expressed shRNA vectors also induced the same phenotype in JuB2 cells and other HSA cell lines such as JuB4, Re21, and Ud6 (Figs. 5A and 5B). These results suggest that KDM2B is an important histone demethylase in HSA cell survival. To examine whether KDM2B can alter global histone methylation and ubiquitination levels in HSA cell lines, I performed western blotting for histone methylations and ubiquitination which can be modified by KDM2B itself or complexes containing KDM2B. I found that H2AK119ub1 levels were globally decreased in KDM2B knockdown cells while other histone modifications were not affected (Fig. 3E). Next, to investigate which KDM2B domain is responsible for HSA cell viability, I rescued KDM2B function in KDM2B silenced HSA cells. I expressed wild type (WT) canine KDM2B with silent mutations for the sequences which were targeted by the shRNAs, and KDM2B mutants with a point mutation for the JmjC domain ($KDM2B^{H283Y}$), the CXXC domain ($KDM2B^{C586A}$), or with PHD-finger domain deleted ($KDM2B^{\Delta PHD}$) (Tzatsos et al., 2009; Wang et al., 2011). Overexpression of WT KDM2B and $KDM2B^{C586A}$ mutant but not the

KDM2B^{H283Y} nor the KDM2B$^{\Delta PHD}$ mutants rescued the phenotype (Fig. 3F), which suggests that the JmjC and the PHD-finger domains are important for the KDM2B function in HSA.

To verify our *in vitro* results and to know the effect of KDM2B silencing *in vivo*, JuB2 cells with Dox-inducible shRNAs for KDM2B or the scramble shRNA were injected subcutaneously into nude mice and the tumor volumes over time were measured. Dox-containing food pellets were provided to the mice to induce shRNA expression when the largest tumor reached 150 mm^3 in volume. Tumor xenografts started to decrease in volume four days after induction of KDM2B silencing, moreover, half of the xenografts bearing shKDM2B-A and one out of eight xenografts bearing shKDM2B-C completely regressed ten days post-induction (Figs. 3G and 3H). At the endpoint, tumor xenografts with silenced KDM2B had significantly decreased tumor weights compared with the xenografts overexpressing the scramble shRNA control (Fig. 3I). I also xenografted JuB2 cells expressing the silencing vector for KDM1A or KDM2A. Although tumor volume repression was initially observed post-doxycycline treatment, tumor regrowth was observed ten days post-doxycycline treatment signifying that other histone demethylases or proteins can rescue KDM1A or KDM2A function *in vivo* or some cell populations were not affected by their knockdown (Fig. 3G).

These results suggest that KDM2B is important for HSA cell survival both *in vitro* and *in vivo* and its local catalytic activity is responsible for the phenotype.

KDM2B knockdown induces apoptosis via accumulation of DNA damages

To understand the mechanisms by which KDM2B regulates HSA cell survival, I performed RNA-seq followed by gene set enrichment analysis (GSEA) in JuB2 cells expressing shKDM2B-A versus JuB2 cells expressing scrRNA-1. Silencing of KDM2B showed negative correlations with angiogenesis and glycolysis pathways, which might reflect decreased HSA cell viability (Fig. 7A). Interestingly, expressions of genes downregulated in response to ultraviolet (UV) radiation (HALLMARK_UV_RESPONSE_DN) were decreased by KDM2B knockdown (Fig. 6A). Considering this correlation and the fact that UV response can trigger DNA damage response (Stokes et al., 2007), we speculated that DNA damage might be related to KDM2B knockdown phenotypes. This speculation was further supported by positive

enrichment of the G2M checkpoint and the interferon response pathways, which have been reported to be associated with mitochondrial and nuclear DNA damages (Fig. 7A) (Brzostek-Racine et al., 2011; J. Chen et al., 2020; Mboko et al., 2012). These results were validated by qRT-PCR (Figs. 6B, 7B-E). Next, I performed Cleavage Under Target & Release Using Nuclease (CUT&RUN) to examine whether H2AK119ub1 and H3K4me3 levels at the promoters or gene bodies of *GAPDH*, *KDM2B*, and *KDM2B* target genes (*INSIG1* and *OAS2*) were affected by KDM2B knockdown. Consistent with global decrease in H2AK119ub1 by KDM2B knockdown, I found that H2AK119ub1 at the promoter regions of *GAPDH* and *OAS2* were significantly decreased in KDM2B knockdown cells while H2AK119ub1 at the gene bodies were not affected (Fig. 6C). H3K4me3 levels at the promoter regions were decreased in *GAPDH* and *INSIG1* and increased in *OAS2* in KDM2B knockdown cells, which was consistent with their gene expression changes (Figs. 6B, 6C, 7B). To further dissect the mechanism, I examined the expression levels of proteins involved in DNA repair pathway. Total ATM, c-FOS, and γH2A.X expressions were upregulated in HSA cell lines compared to CnAOEC and their expressions were significantly decreased by KDM2B knockdown (Figs. 6D and 6E). Phosphorylated-ATM (pATM), an active form of ATM, was also decreased by KDM2B knockdown. Next, I carried out alkaline comet assay to detect DNA strand breaks in HSA cell lines upon KDM2B silencing. Our results showed that KDM2B silencing drastically increased tail DNA percentages, tail lengths, and tail momentums compared to the scramble control (Figs. 6F and 6G). Furthermore, flow cytometry analysis using PI revealed that JuB2 with silenced KDM2B increased aneuploid peaks although parental HSA cells also showed aneuploidy (Figs. 8A, 8B, 9A, 9B). In contrast, overexpression of WT KDM2B in JuB2 HSA cells resulted to significantly decreased aneuploid cell population compared to empty vector (EV) expressing JuB2 cells (Figs. 9C and 9D). In addition, active apoptosis markers, cleaved-caspase 3, BAX, and phosphorylated ERK1/2 (pERK1/2), were increased in cells with silenced KDM2B compared to the scramble control cells (Fig. 9E). Furthermore, overexpression of KDM2B in CnAOEC decreased the pERK1/2 expression compared to the EV control (Fig. 9F and 9G) and repressed mRNA expressions of cell cycle checkpoint genes such as p15ink4b, p16ink4a, and ATR (Fig. 9H). These results suggest that KDM2B knockdown in HSA cells induces cell death via apoptosis caused by the accumulation

of DNA damages due to the low expression of proteins involved in DNA repair.

KDM2B is highly expressed in clinical cases of HSA

I demonstrated that KDM2B upregulation was important for HSA cell survival, but KDM2B expression in clinical HSA cases has not been investigated. To this end, I analyzed seventeen clinical cases of HSA and compared the immunohistochemical KDM2B expression between HSA cells and normal endothelial cells in the same sample. Our results showed that KDM2B was highly expressed in HSA cells compared to normal endothelial cells in almost all the cases examined regardless of proliferation patterns or degree of differentiation (Figs. 10A and 10B). The average KDM2B score in HSA cells was significantly higher than that in normal endothelial cells (Fig. 10C). I then also examined the benign endothelial tumor, hemangioma (HMA), for KDM2B expression. Interestingly, KDM2B expression levels in hemangioma cells were likely lower than normal endothelial cells in the same sample ($P = 0.096$; Figs. 10D-F,). The average KDM2B expression scores in HSA were significantly higher than in HMA cells when the average KDM2B scores in tumor cells were normalized to normal endothelial cells in the same slides (Fig. 10G). KDM2B expressions were also analyzed in histologically-similar tumors, hemangiopericytoma (HPC), melanoma, and fibrosarcoma cells. Results showed that HPC, melanoma, and fibrosarcoma cells had similar KDM2B expression compared to normal endothelial cells in the same slide (Figs. 11A–11C). These results suggest that KDM2B expresses in clinical HSA samples and can be used as a biomarker to differentiate HSA and HMA. In addition, KDM2B may also be used as a molecular marker to differentiate HSA from HPC, melanoma, and fibrosarcoma.

GSK-J4 inhibits HSA cell viability

I demonstrated that KDM2B inhibition through shRNA could induce HSA cell death. Based on this, I hypothesized that pharmacological KDM2B inhibition could also induce HSA cell death. To test this hypothesis, I used a histone demethylase inhibitor GSK-J4 since there is no KDM2B specific KDM2B inhibitor available. I treated HSA cell lines with different concentrations of GSK-J4 and compared it to doxorubicin-treated cells. GSK-J4 inhibited HSA cell viability at a lower concentration in JuB2, JuB4, and Ud6 cell lines compared to doxorubicin (Fig. 12A). HSA cell lines treated with GSK-J4

have higher expressions of cleaved-caspase 3 compared to HSA cells treated with doxorubicin. In contrast, GSK-J4-treated HSA cells have decreased t-ATM and γH2A.X expression compared to DMSO control-treated HSA cells (Fig. 12B). Global H3K4me3 level was increased four days after GSK-J4 treatment while H3K79me3, H3K36me2/3, and H3K27me3 were not globally changed (Fig. 13A).

To determine whether GSK-J4 can be used as an alternative drug for HSA treatment, I treated nude mice harboring JuB2 tumors with DMSO, GSK-J4 or doxorubicin. GSK-J4 treatment significantly decreased the tumor growth over time and tumor weights at the endpoint compared to DMSO treatment (Figs. 12C–E). Although Doxorubicin treatment also led to decreased tumor growth, it had significant toxicity and led to 83% mortality in 21 days (Fig. 12F). In contrast, GSK-J4 did not induce any death during the treatment period. Body and liver weights decreased in doxorubicin-treated mice compared to DMSO or GSK-J4 treated mice (Figs. 12G and 13B). In addition, increased hematopoiesis in bone marrow, a sign of myelosuppression, and dilation of intestines were only observed in mice treated with doxorubicin (Figs. 13C and 13D). These results suggest that GSK-J4 can selectively inhibit HSA cell growth by inducing HSA cell apoptosis without any obvious side-effects. Thus, GSK-J4 could be used as a therapeutic alternative to doxorubicin for HSA treatment.

Discussion

To our knowledge this is the first study which evaluated the role of epigenetic regulators in HSA. I demonstrated that KDM2B upregulation in HSA cell lines and clinical samples is important for HSA cell survival by regulating DNA damage repair and apoptosis. There are three possible reasons for the high expression of KDM2B in HSA. Firstly, KDM2B upstream regulators may be dysregulated. In bladder cancer, the upregulation of fibroblast growth factor-2 upregulated the KDM2B/EZH2-miR-101 pathway and promoted tumor cell proliferation, survival, and migration (Kottakis et al., 2011). In squamous cell and cervical carcinomas, increased copy number of *MYC* resulted to increased KDM2B expression (Peta et al., 2018). Secondly, the KDM2B gene itself may have acquired increased copy numbers. I demonstrated that parental HSA cell lines contain an aneuploid cell population. Since cell aneuploidy can cause

genomic instability as a result of decreased DNA damage repair activity (Sheltzer et al., 2011), some genes including KDM2B in HSA might have increased copy numbers. Lastly, KDM2B might be upregulated to compensate for DNA damage and to integrate genetic stability in HSA genomes. As I mentioned above, flow cytometry analysis revealed multiple aneuploid peaks in HSA cell lines. Aneuploidy has also been reported in clinical cases of HSA and in HSA cell lines, which implies that HSA cells are subject to high level cellular stress (Fosmire et al., 2004; Thomas et al., 2014; Zhu et al., 2018). In such conditions, HSA cells may bypass cell death caused by accumulated cellular stresses through modulation of gene expression. I showed that knockdown of KDM2B in HSA cell lines decreased DNA repair protein expressions and increased DNA damage. In contrast, exogenous expression of KDM2B in JuB2 and in CnAOEC increased euploid population and inhibited apoptosis, respectively. KDM2B may ease cellular stress caused by DNA damage in endothelial cells by regulating the DNA repair system.

KDM2B knockdown decreased global H2AK119ub1 levels (Fig. 3E) and H2AK119ub1 was enriched at the promoter regions of *GAPDH* and *OAS2* (Fig. 6C). H2AK119ub1 at the promoter regions is established by non-canonical PRC1.1(Boom et al., 2016). KDM2B is the DNA-binding subunit of non-canonical PRC1.1, which does not work with PRC2 complex which catalyzes H3K27 methylation (Boom et al., 2016). Since H2AK119ub1 was enriched at the promoter regions of *GAPDH* and *OAS2*, and KDM2B knockdown did not change H3K27me3 levels in HSA cells, non-canonical PRC1.1 might be important for HSA cell survival.

KDM2B and other histone demethylases are known to have a double-edged function in cancer (Yan et al., 2018b). A study showed that KDM2B suppresses tumorigenesis in gastric cancer by enhancing c-FOS degradation, and that impairment of KDM2B through patient-derived mutations enhances tumor cell proliferation (Han et al., 2016). In contrast, degradation of c-FOS by KDM2B in glioblastoma multiforme can increase cancer cell resistance to chemotherapy (Kurt et al., 2017). In HSA, I showed that positive regulation of DNA repair genes by KDM2B can enhance HSA cellular viability in contrast to a previous report where KDM2B was shown to promote colon cancer cell survival by negatively regulating DNA damage response-related genes such as ATM and ATR (L. Chen et al., 2014). These contrasting evidences support the role

of KDM2B in DNA damage response and suggest that the role of KDM2B in DNA damage response in cancer cells is highly context dependent.

Figures

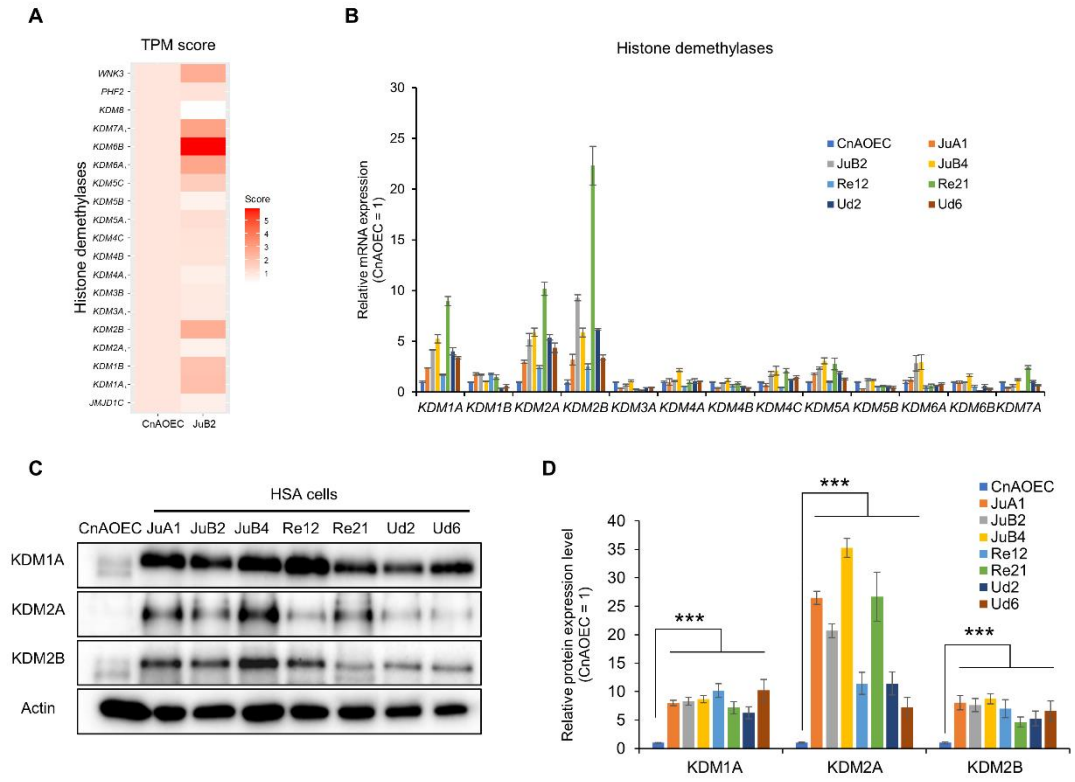

Fig. 1. Epigenetic regulators are dysregulated in HSA.

A, Transcripts per million (TPM) scores of histone demethylases in CnAOEC and JuB2 HSA cell line. **B**, qRT-PCR verification of select histone demethylases in CnAOEC and HSA cell lines. **C**, Western blotting for KDM1A, KDM2A, and KDM2b in CnAOEC and HSA cell lines. **D**, Quantitative analysis of KDM1A, KDM2A, and KDM2B protein expressions in CnAOEC and HSA cell lines. Data are presented as mean values ± SD, standard deviation ***, $P < 0.001$, Tukey's test.

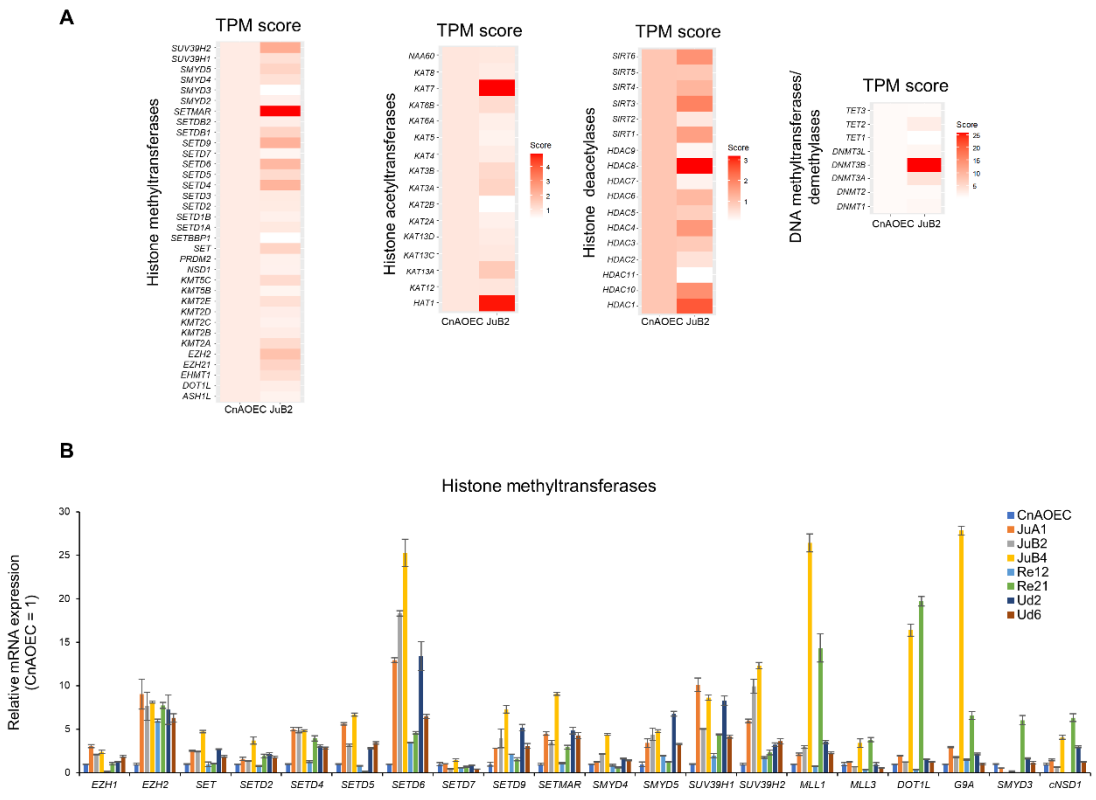

Fig. 2. Histone methyltransferases are differentially expressed in HSA.

A, TPM scores of histone methyltransferases, histone acetyltransferases, histone deacetylases, DNA methyltransferases, and DNA demethylases in CnAOEC and JuB2 HSA cell line. **B**, qRT-PCR verification of select histone methyltransferases in CnAOEC and HSA cell lines. Data are presented as mean values ± s.d.

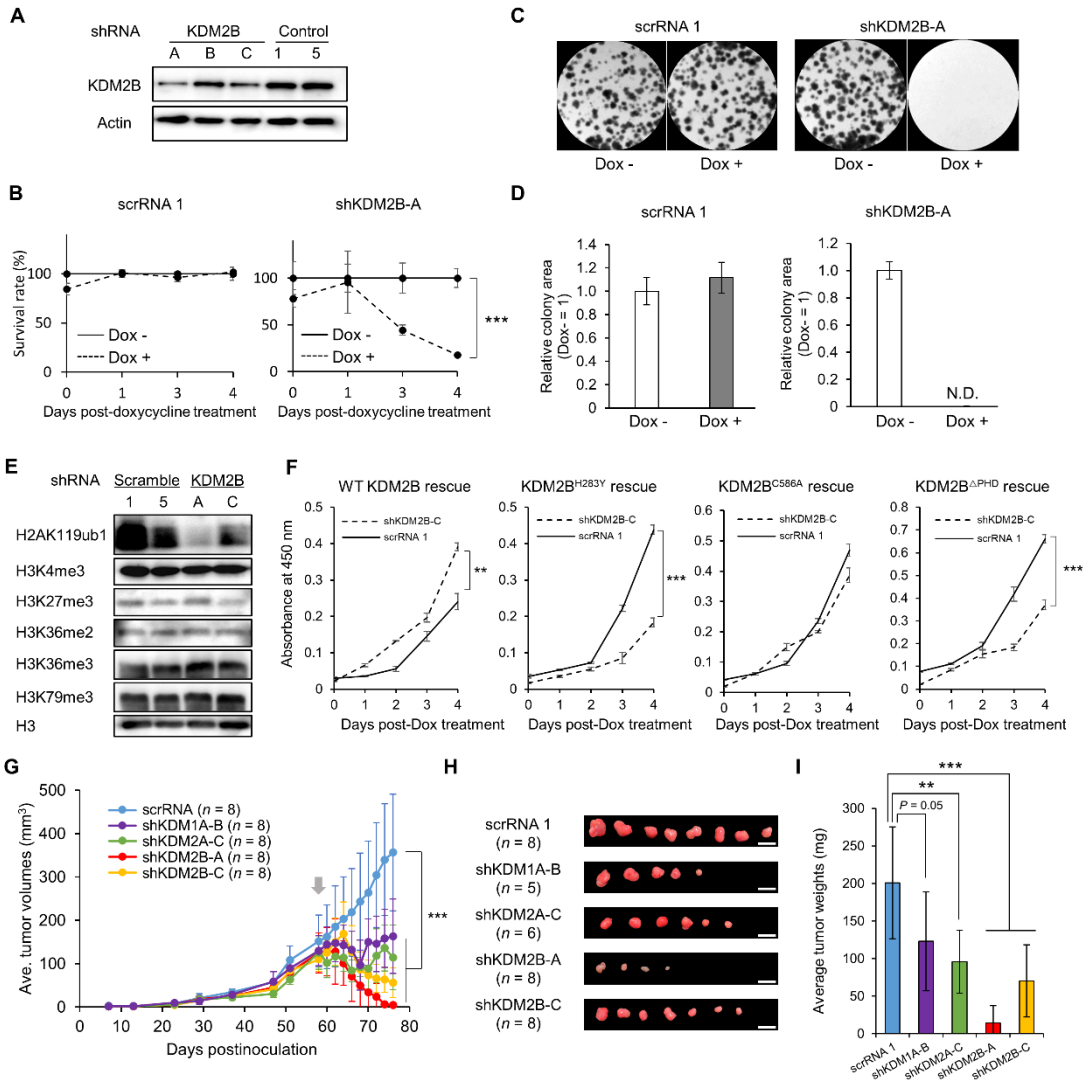

Fig. 3 KDM2B is important for HSA cell survival in vitro and in vivo.

A, Western blotting of KDM2B to verify the silencing efficiency of shRNA vectors developed for Kdm2b. **B**, Cell viability analysis after the induction of the inducible shRNA vector using doxycycline. Data are presented as mean values ± s.d. ***P<0.001, Two-way ANOVA. **C**, Colony formation assay of JuB2 cells after KDM2B silencing. **D**, Quantitative analysis of C. N.D. means not detected. **E**, Western blotting of histone modifications. **F**, Cell viability analysis after rescue overexpression of WT KDM2B, or dominant negative mutants for the JmjC (KDM2B^{H283Y}), CxxC (KDM2B^{C586A}), or PHD (KDM2B$^{\triangle PHD}$) domains. **, P < 0.01; ***, P < 0.001, two-way ANOVA. **G**, Tumor growth at different time points before and after the induction of the

shRNA expression in JuB2 cells inoculated in nude mice. ***$P < 0.001$, two-way ANOVA with Dunnett's post-hoc test for tumor volumes after starting doxycycline treatments (arrow). **H** and **I**, Tumor sizes and weights of tumors harboring scramble RNA or shRNA for KDM1A, KDM2A, or KDM2B 78 days after tumor transplantation. Scale bars, 1 cm. ** $P < 0.01$ *** $P < 0.001$, Dunnett's test. Data are presented as mean values ± s.d.

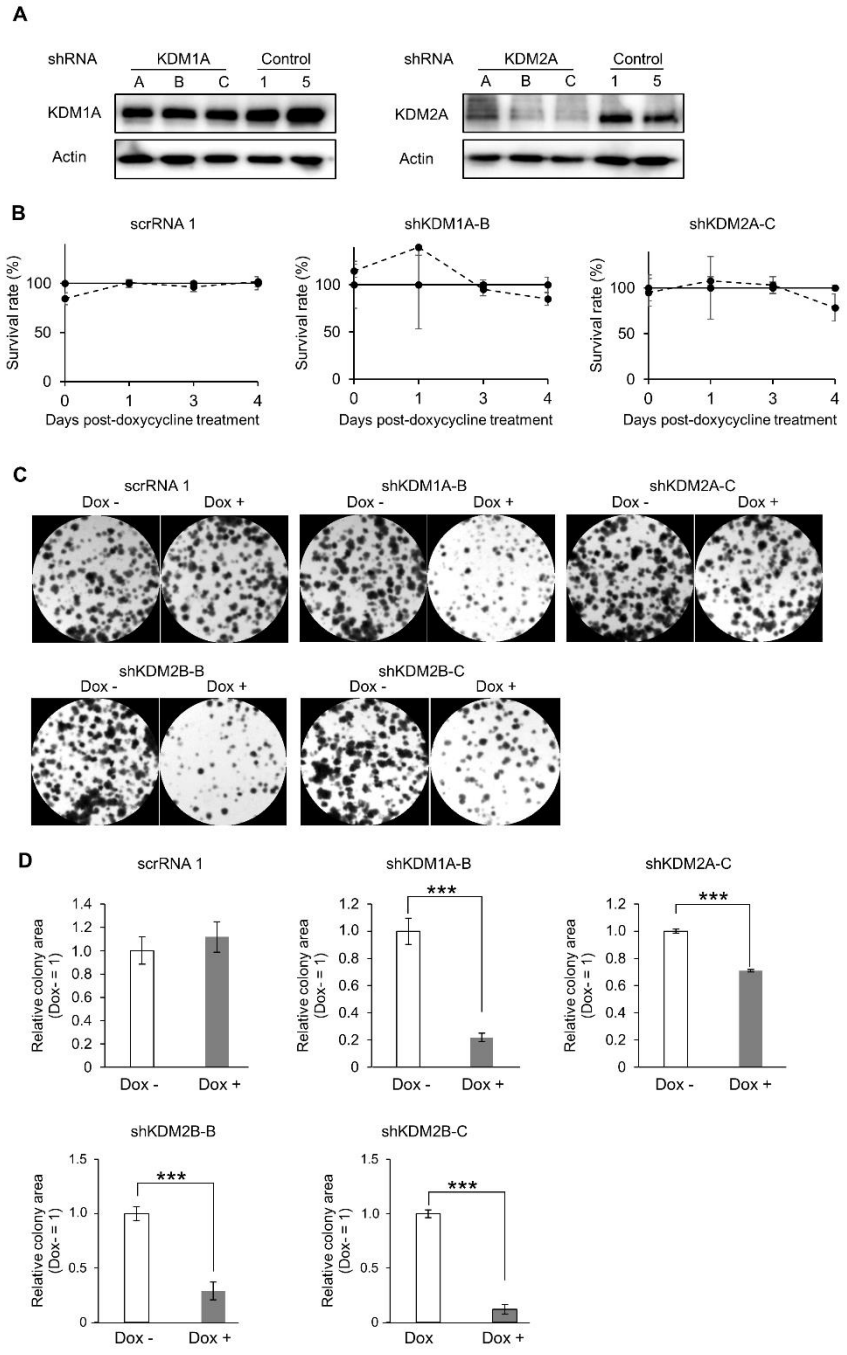

Fig. 4. KDM2B is important for HSA cell survival *in vitro*.

A, Western blotting of KDM1A and KDM2A to verify the silencing efficiency of shRNA vectors developed for KDM1A and KDM2A. **B,** Cell viability analysis after the induction of the inducible shRNA vector using doxycycline. **C,** Colony formation assay

of JuB2 cells after KDM1A, KDM2A, or KDM2B silencing. **D,** Quantitative analysis of **C**. N.D. means not detected. ***P<0.001, Student-*t* test.

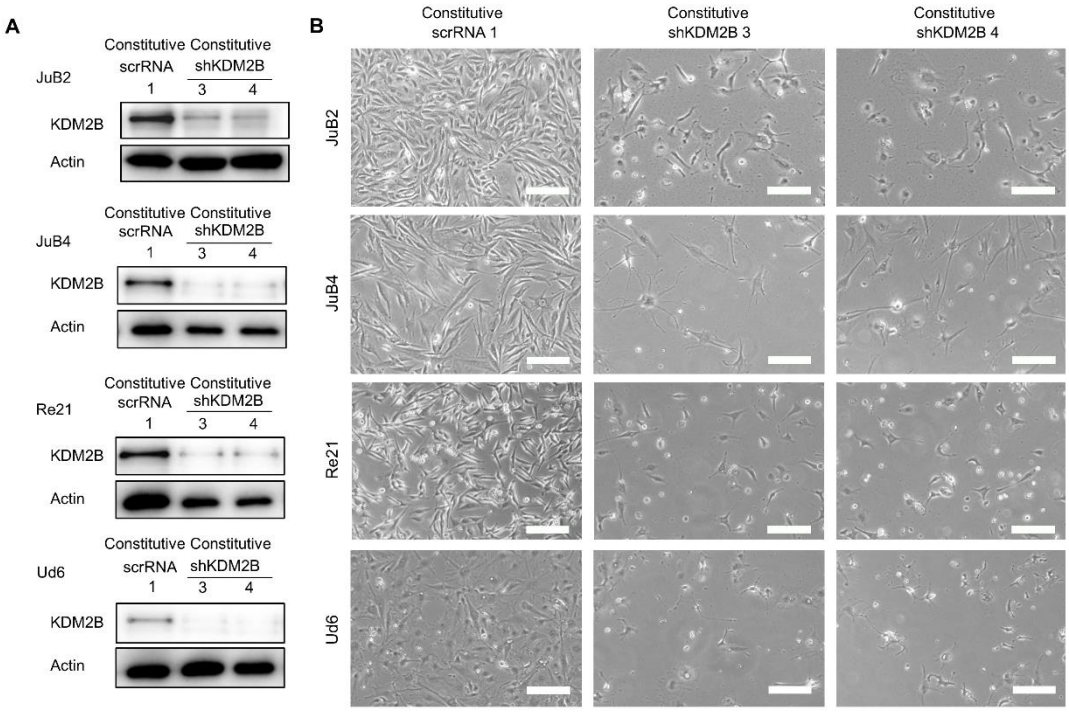

Fig. 5. KDM2B is also essential in different HSA cell lines.

A, Western blotting for KDM2B following KDM2B knockdown with constitutively expressed silencing vectors. **B**, Viability and morphology of JuB2, JuB4, Re21, and Ud6 HSA cell lines 4 days after silencing of KDM2B. Scale = 100 μm.

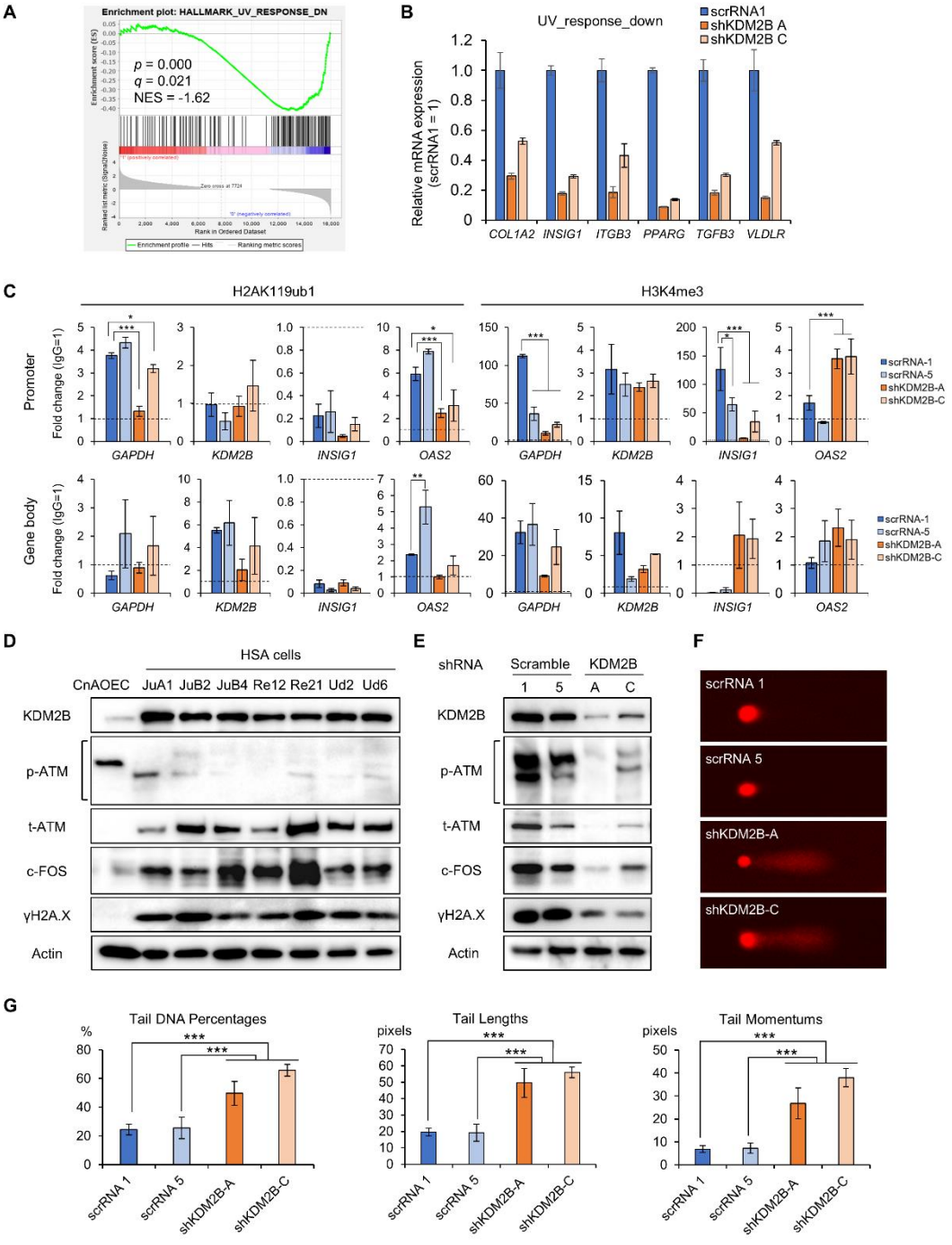

Fig. 6 KDM2B positively regulates DNA repair pathway.

A, GSEA enrichment plot for UV_Response_DN in shKDM2B-A versus scrRNA-1. **B**, qRT-PCR verification of gene expressions listed in UV_Response_DN gene set. **C**, H2AK119ub1 and H3K4me3 enrichment at promoters or gene bodies. Results are

indicated as fold changes normalized by IgG control samples. Dotted lines indicate IgG control sample =1. Data are presented as mean values ± s.d. *** $P < 0.001$, ** $P < 0.01$, * $P < 0.05$, Dunnett's test. **D** and **E**, Western blotting for Atm, c-Fos, and γH2A.X in normal endothelial cells and HSA cell lines (D) and in JuB2 cells expressing shRNA control or shKDM2B (E). **F**, Representative images of alkaline comet assays in scrRNA or shKDM2B JuB2 cells. **G**, Tail DNA percentages, lengths, and momentums of JuB2 HSA cells harboring scrRNA or shRNA for KDM2B. Data are presented as mean values ± s.d. *** $P < 0.001$, Tukey's test.

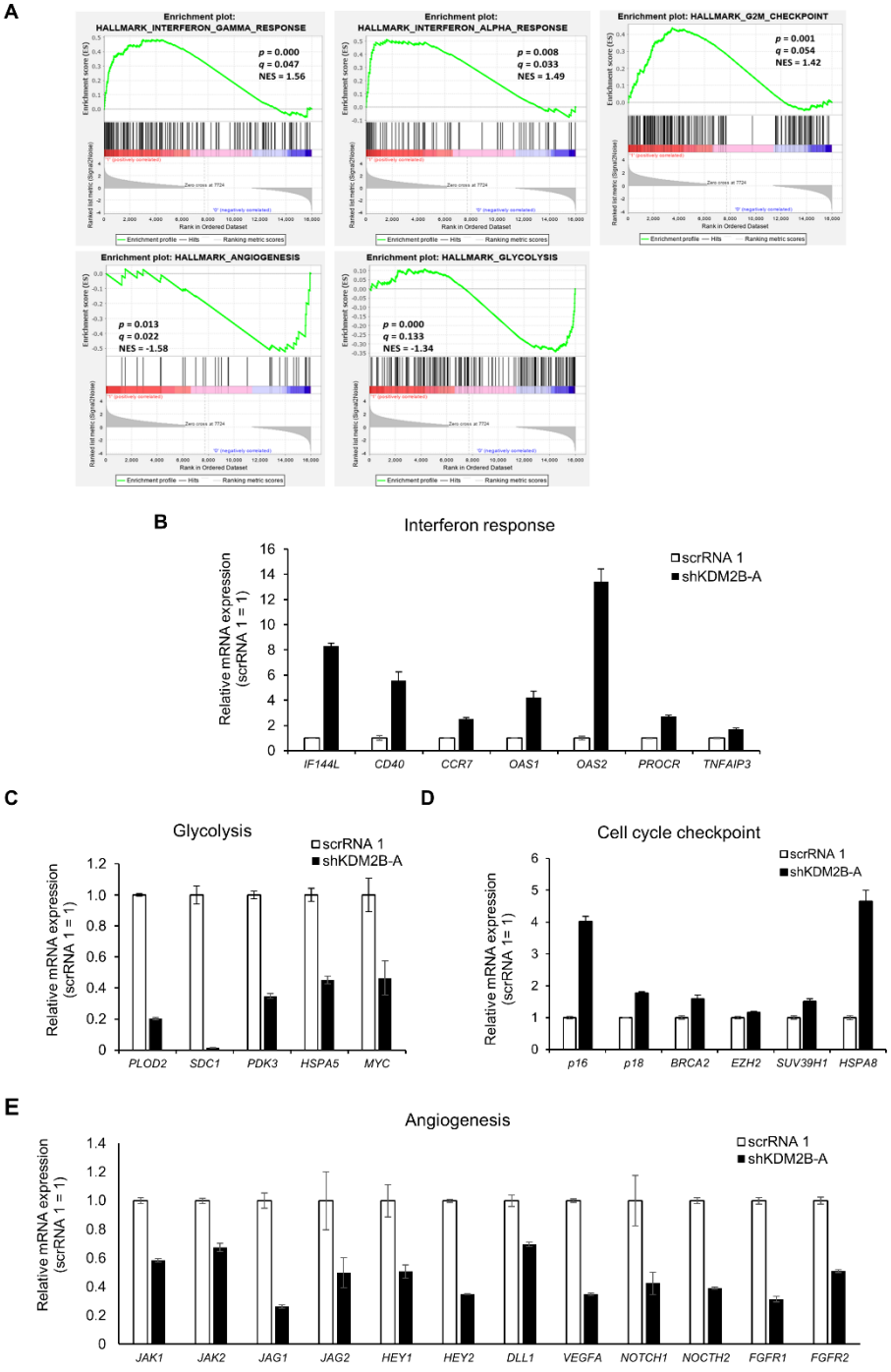

Fig. 7. KDM2B regulates the interferon responses, cell cycle checkpoints, angiogenesis, and glycolysis pathways.

A, GSEA enrichment plots in shKDM2B-A JuB2 cells versus scrRNA-1 JuB2 cells. **B** to **F**, qRT-PCR results of genes related to the enriched pathways in a. Data are presented as mean values ± s.d.

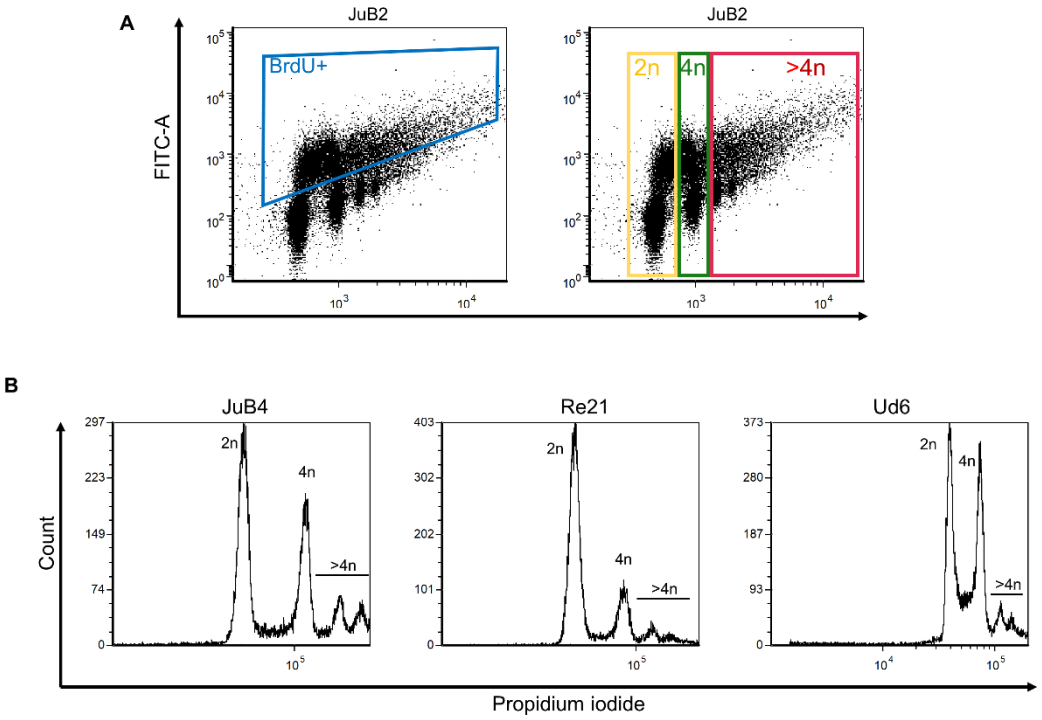

Fig. 8. Parental HSA cells are aneuploid.

A, Dot plots illustrating the gating methods for 2n, 4n, > 4n, and dividing cell populations. **B**, Histograms of propidium iodide intensities in JuB4, Re21, and Ud6 cell lines.

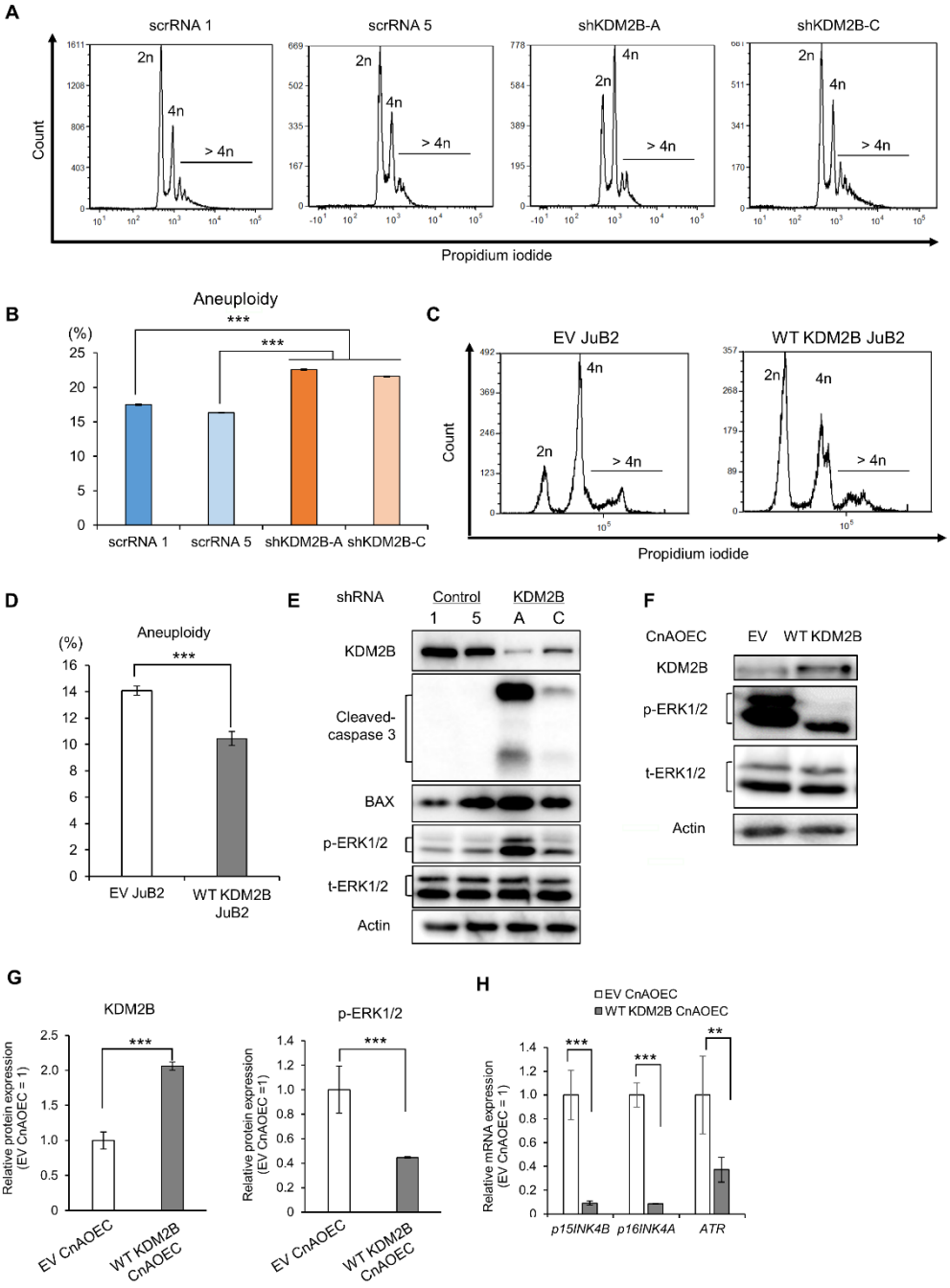

Fig. 9 Kdm2b regulates aneuploidy and apoptosis in HSA.

A, Histograms of PI intensities in scrRNA and shKDM2B JuB2 cells. **B,** Percentages of aneuploid cells in shRNA and shKDM2B JuB2 cells. *** $P < 0.001$, Tukey's test. **C,** Histograms of PI intensities in EV infected JuB2 cells and WT KDM2B JuB2 cells. **D,**

Percentages of aneuploid cells in EV JuB2 and WT Kdm2b JuB2. ** $P < 0.001$, Student-*t* test. **E,** Western blotting for cleaved-caspase 3, Bax and Erk 1/2 in JuB2 HSA cells expressing scrRNA controls or shKDM2B RNAs. KDM2B and Actin images are the same as Fig. 3E because we used the same samples. **F,** Phase contrast images of CnAOEC cells infected with EV or overexpressing WT KDM2B at day 1 and day 19. Scale = 100 µm. **G,** Western blotting of Erk 1/2 in CnAOEC infected with EV or overexpressing WT KDM2B. **H,** Quantification of KDM2B and phosphorylated Erk 1/2 expression in EV infected or WT KDM2B expressing CnAOEC normalized with Actin and total Erk 1/2, respectively. **I,** qRT-PCR analysis of cell cycle related genes after overexpression of WT KDM2B in normal endothelial cells. Data are presented as mean values ± s.d. ** $P < 0.01$ *** $P < 0.001$, Student's *t*-test.

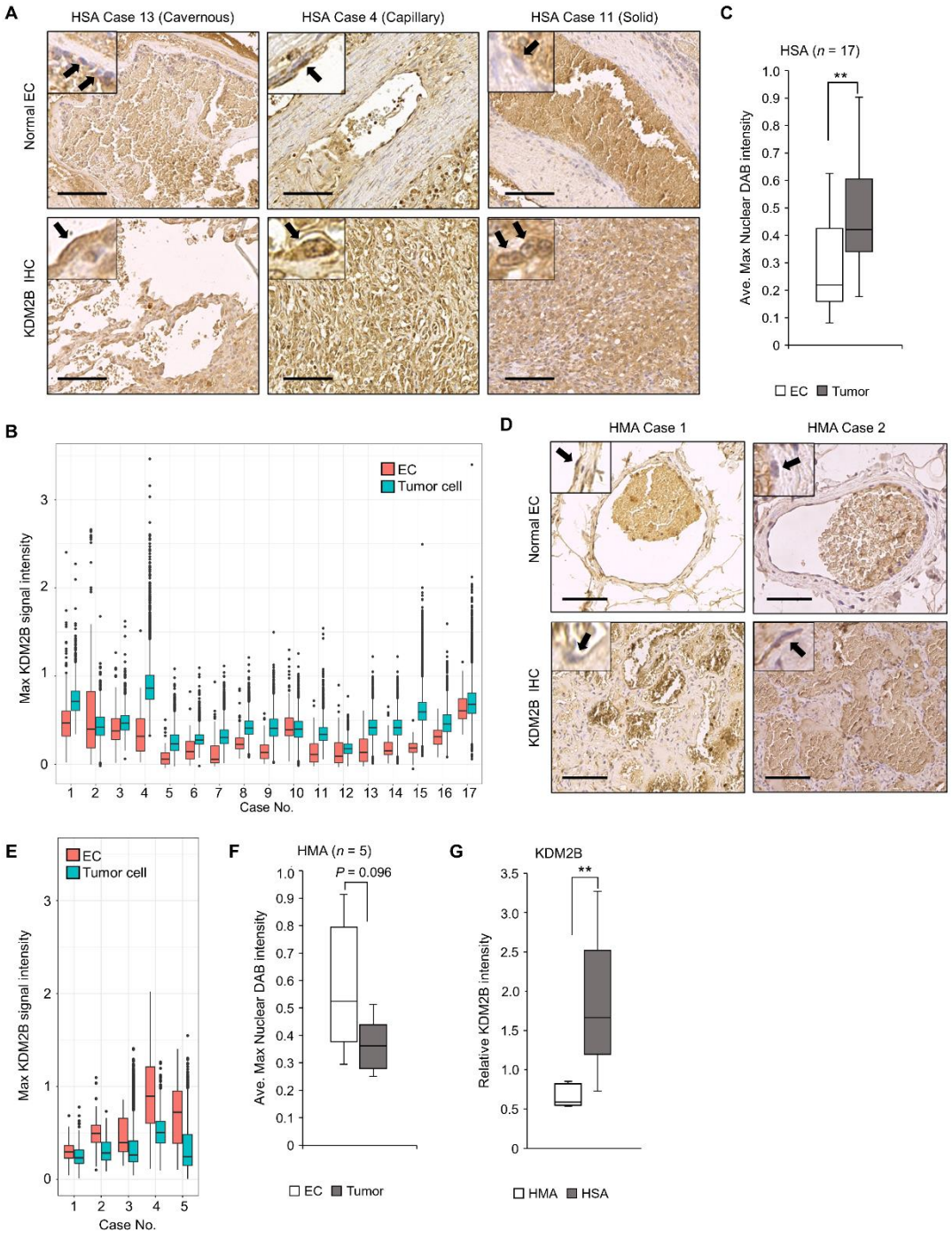

Fig. 10 KDM2B can be used as a differential biomarker for HSA.

A, Representative images of immunohistochemistry (IHC) for clinical HSA samples. Top: Normal endothelial cells (EC) in the healthy region. Bottom: HSA tumor cells in the tumor region. Inserted pictures are magnified views and arrows indicate EC and

tumor cells. Proliferation patterns are indicated with case numbers. Scale = 100 μm. **B**, Max nuclear DAB intensities in individual endothelial cells (EC) and tumor cells (Tumor) of each HSA case. **C**, Average max nuclear DAB intensities of EC and tumor cells in each HSA case. **D**, Representative IHC images of hemangioma (HMA), a benign endothelial cell tumor. Top: EC in the healthy region. Bottom: HSA tumor cells in the tumor region. Inserted pictures are magnified views and arrows indicate EC and tumor cells. Scale = 100 μm. **E**, Max nuclear DAB intensities in individual EC and tumor cells of each HMA case. **F**, Average max nuclear DAB intensities of EC and tumor cells in each HMA case. **G**, Comparison of relative KDM2B intensity of HSA and HMA cells normalized by normal endothelial cells in their respective slides. Data are presented as mean values ± s.d. ** P <0.01, Student's t-test.

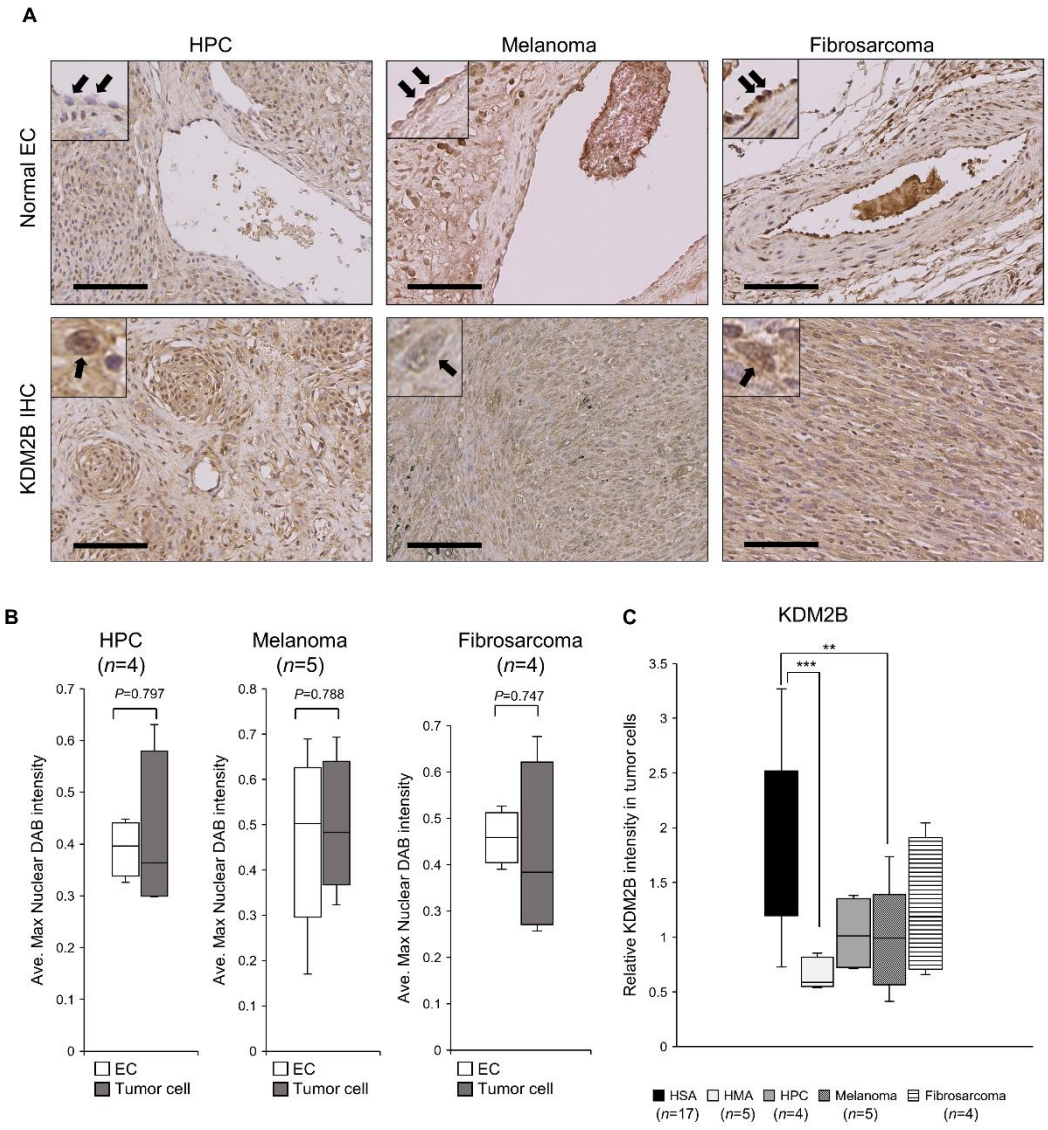

Fig. 11. KDM2B expression can be used as a biomarker for endothelial cell tumors. A, Representative images of IHC analyses for clinical cases of HPC (n=4), melanoma (n=5), and fibrosarcoma (n=4). Top: Normal endothelial cells (EC) in the healthy region. Bottom: tumor cells in the tumor region. Inserted pictures are magnified views and arrows indicate EC and tumor cells. Scale = 100 μm. **B**, Average maximum nuclear DAB intensity in each HPC, melanoma, and fibrosarcoma case. **C**, Comparison of the relative Kdm2b intensities in tumor cells normalized by average Kdm2b intensities in EC on the same slides between HSA, HMA, HPC, melanoma, and fibrosarcoma. Data presented as mean values ± s.d. $^{**}P < 0.01$, Bonferroni test.

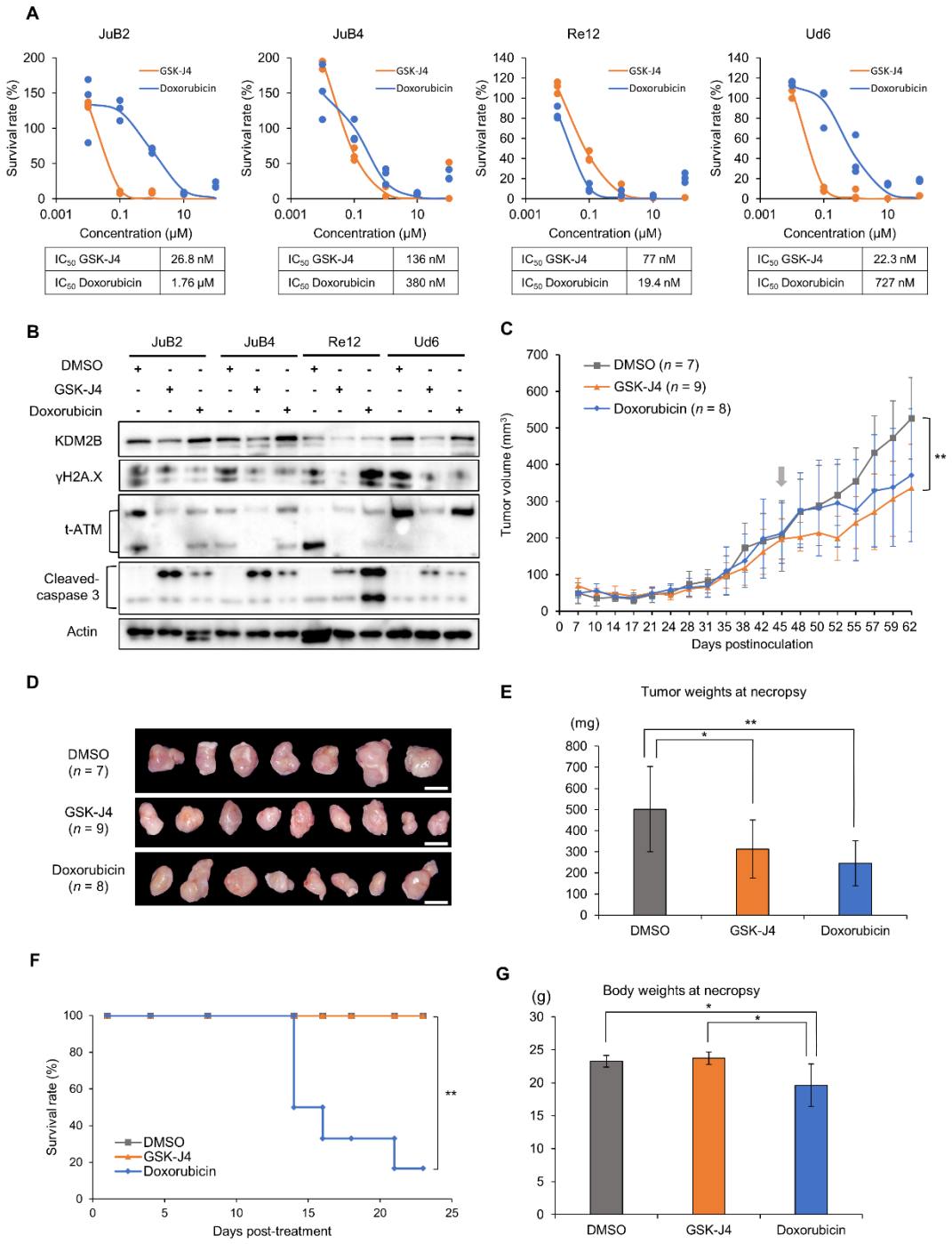

Fig. 12 GSK-J4 inhibits HSA cell proliferation *in vitro* and *in vivo*.

A, Survival rates and IC50 values of GSK-J4 or doxorubicin-treated HSA cell lines. **B**, Western blotting for γH2A.X, Atm and cleaved-caspase 3 in HSA cells treated with

GSK-J4 or doxorubicin. **C**, Tumor growth curves of JuB2 HSA cell xenografts in nude mice. Treatment with DMSO, GSK-J4, or doxorubicin started at day 45 (arrow). n indicates the number of mice. $^{**}P < 0.01$, two-way ANOVA with Dunnett's post-hoc test. **D**, Gross images of collected tumors at day 64. n indicates the number of collected tumors. **E**, Tumor weights of DMSO, GSK-J4, or doxorubicin-treated nude mice at necropsy. **F**, Kaplan-Meier survival curves of DMSO, GSK-J4, or doxorubicin-treated nude mice after starting treatments. $^{**}P < 0.01$, Log-rank test. **G**, Body weights of DMSO, GSK-J4, or doxorubicin-treated nude mice at necropsy. Data are presented as mean values ± s.d. $^{**}P < 0.01$, Tukey's test.

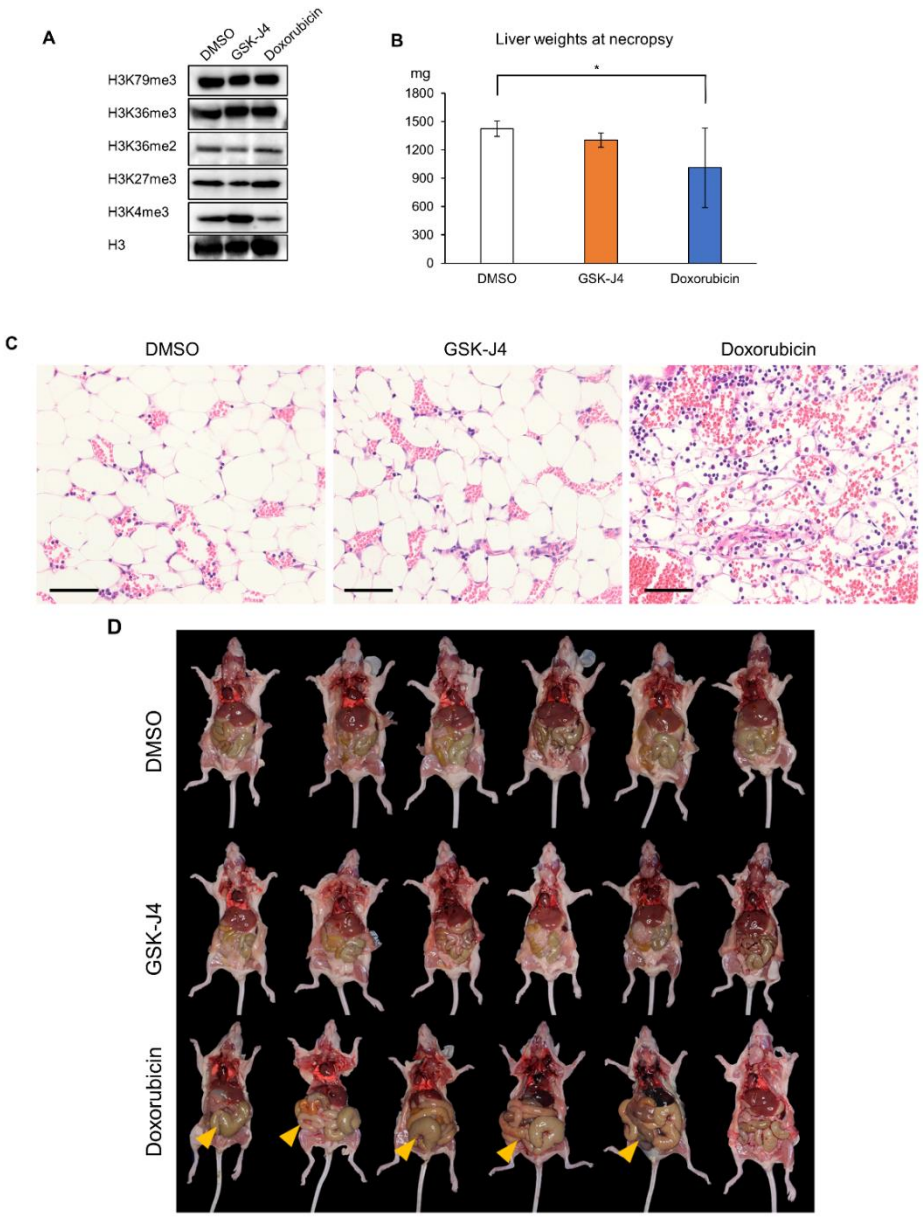

Fig. 13. GSK-J4 can be used as a therapeutic alternative to doxorubicin treatment in HSA.

A, Western blotting for histone lysine methylations 4 days after GSK-J4 treatment. **B**, Liver weights of mice treated with DMSO, GSK-J4, or doxorubicin. Data are presented as mean values ± s.d. *P < 0.05, Tukey's test. **C**, Representative images of bone marrow sections from mice treated wih DMSO, GSK-J4, or doxorubicin. Scale = 100 μm. **D**, Gross images of nude mice treated with DMSO, GSK-J4, or doxorubicin. Arrowheads indicate enlargement of intestinal segments.

Tables

Table 1. List of antibodies used in the study.

Protein Name	Catalog Number	Maker	Host	Dilution
KDM1A	2139S	Cell Signaling Technology	Rabbit	1:1000
KDM2A	ab191387	Abcam	Rabbit	1:1000
KDM2B	sc-293279	Santa Cruz Biotechnology, Inc.	Mouse	1:1000
ACTIN	MAB1501	Sigma-Aldrich	Mouse	1:1000
P-ATM	sc-47739	Santa Cruz Biotechnology, Inc.	Mouse	1:1000
t-ATM	sc-377293	Santa Cruz Biotechnology, Inc.	Mouse	1:1000
C-FOS	sc-166940	Santa Cruz Biotechnology, Inc.	Mouse	1:1000
γH2A.X	A300-081A-T	Bethyl Laboratories, Inc.	Rabbit	1:1000
CLEAVED-CASPASE 3	9661S	Cell Signaling Technology	Rabbit	1:1000
P-ERK1/2	4370S	Cell Signaling Technology	Rabbit	1:1000
T-ERK1/2	4695S	Cell Signaling Technology	Rabbit	1:1000
H3K79me3	74073S	Cell Signaling Technology	Rabbit	1:1000
H3K36me3	ab9050	Abcam	Rabbit	1:1000
H3K36me2	39255	Active Motif	Rabbit	1:4000
H3K27me3	ab6002	Abcam	Mouse	1:1000
H3K4me3	301-34811	Fujifilm Wako	Mouse	1:1000
H2AK119ub1	8240S	Cell Signaling Technology	Rabbit	1:2000
H3	39140	Active Motif	Rabbit	1:5000
ANTIRABBIT	NA934VS	Sigma-Aldrich	Donkey	1:10000
ANTIMOUSE	G21040	Thermo Fisher Scientific	Goat	1:10000

Table 2. List of qRT-PCR primers used in the study.

Species	*Target*		Sequence	Gene ID	Reference
Canine	*TBP*	F	ATAAGAGAGCCCCGAACCAC	ENSCAFG00000004119	Peters *et al.*, 2007
		R	TTCACATCACAGCTCCCCAC		
	KDM1A	F	CCCACCTGAGGAAGAAAATG	ENSCAFG00000013361	Gulay et al., 2021
		R	GGAAAACAGGCTGCTTCTTG		
	KDM2A	F	AAGAAATGTGTCCCCACAGG	ENSCAFG00000011792	Gulay et al., 2021
		R	CAAGCTCCTCCAGCAAAATC		
	KDM2B	F	AGAAGCCACGAATGCCATTG	ENSCAFG00000008259	Gulay et al., 2021
		R	AACAGCCTTTCACGCTCATC		
	KDM3A	F	ACTTTAGGATGCCGGTCACAG	ENSCAFG00000007522	Gulay et al., 2021
		R	TGCAGCTTCTTGAGTTTGGC		
	KDM4A	F	GATTTCCCCTTTGATGCTGA	ENSCAFG00000004903	Gulay et al., 2021
		R	TGGTAGACTCCGCACAGTTG		
	KDM4B	F	CAGTCAGGCCTCTTCACACA	ENSCAFG00000018925	Gulay et al., 2021
		R	CCAATACTTGCGTTCCAGGT		
	KDM4C	F	CCACTGACTCTGGTGAAGCA	ENSCAFG00000001434	Gulay et al., 2021
		R	TCGCCCAAGACTCTGTTTCT		
	KDM5A	F	GGACCTTGAGCCTCTGAGTG	ENSCAFG00000015781	Gulay et al., 2021
		R	GGAATGCATGGCTTCAATCT		
	KDM5B	F	GCTGTCCAACTCCCAAATGT	ENSCAFG00000010452	Gulay et al., 2021
		R	GGCTCTTGGGTTTTTCCTTC		
	KDM6A	F	ATAACCGCACAAACCTGACC	ENSCAFG00000014589	Gulay et al., 2021
		R	AGGACCTGCCAAATGTGAAC		
	KDM6B	F	TCTTCGATTTTCCCCCTACC	ENSCAFG00000016817	Gulay et al., 2021
		R	GAATGGATTCGTCCAGCATC		
	KDM7A	F	AGCAACCAGGCAACAAAAGG	ENSCAFG00000003990	Gulay et al., 2021
		R	TCTTCCCAAGACGCTGTTTG		
	COL1A2	F	TCTCCCTGGTGAATTTGGTC	ENSCAFG00000002069	Gulay et al., 2021
		R	GTTCACCCTTGTTTCCATCG		

	INSIG1	F	TGGGATCACTATTGCCTTCC	ENSCAFG00000005081	Gulay et al., 2021
		R	AGCGGATGTAGAGAAAGTCTGG		
	ITGB3	F	GGATTCCAGCAATGTCCTTC	ENSCAFG00000013735	Gulay et al., 2021
		R	TGGCGTTGAACGATAGAGAC		
	PPARG	F	TTCTCCAGCATTTCCACTCC	ENSCAFG00000004991	Gulay et al., 2021
		R	AGGCTCCACTTTGATTGCAC		
	TGFBR3	F	CACATTGTGCACCAAGAAGG	ENSCAFG00000020179	Gulay et al., 2021
		R	TCATTGAGGCATCCAGTGAG		
	VLDLR	F	GACGAACCCCTGAAAGAATG	ENSCAFG00000002028	Gulay et al., 2021
		R	TGCGCAGTCACATTCATAGC		
	EZH1	F	TGAGGAGTCCCTTTTTCGAG	ENSCAFG00000014827	Gulay et al., 2021
		R	TCATCTGTTGGCAGCTTCAG		
	EZH2	F	CAGACCGGTGAAGAGCTGTT	ENSCAFG00000003411	Gulay et al., 2021
		R	GGGGAGGAAGAGGTAGCAGA		
	SET	F	TCCATCGTCAAAGTCCACTG	ENSCAFG00000032728	Gulay et al., 2021
		R	TCCTGCTGGCTTTATTCTGC		
	SETD2	F	ACAGCAGAAGCAGACACCTC	ENSCAFG00000013392	Gulay et al., 2021
		R	AGGCACTGGACGATGAACTG		
	SETD4	F	TGAATCATAGCCCCGAAGTC	ENSCAFG00000009616	Gulay et al., 2021
		R	AGCCGTTGGTTATCATGAGG		
	SETD5	F	ACCCCCAAACACTACATTCG	ENSCAFG00000005486	Gulay et al., 2021
		R	CCAAGGCTTGCTTTATCCAG		
	SETD6	F	CAAACTCCCCTTTGATGGTG	ENSCAFG00000008461	Gulay et al., 2021
		R	TTTAGGAATGGGCTGAGTGG		
	SETD7	F	AGGTAGCGGTGGGACCTAAT	ENSCAFG00000003703	Gulay et al., 2021
		R	GTTGTAGGGCTCAGGCACAT		
	SETD9	F	AAGGCGCGGTTGTATCTATG	ENSCAFG00000006922	Gulay et al., 2021
		R	TCAATGAGTACCCCATCCAG		
	SETMAR	F	CTTGGAGAACGTGCCTGTGA	ENSCAFG00000005958	Gulay et al., 2021
		R	CAAATGCATCCGGGAAAGGT		
	SMYD3	F	CGGAGATGCAGGAAGTTGGT	ENSCAFG00000029171	

	R	CTCGATGTCTCGGACTGCTC		Gulay et al., 2021
SMYD4	F	TGTGGGAAAGGACCCTAATG	ENSCAFG00000019244	Gulay et al., 2021
	R	AGTGTGAGGCCTTGAATGTG		
SMYD5	F	TGAAGGATCTGGCCTGTATG	ENSCAFG00000008932	Gulay et al., 2021
	R	TGGCTTGATATCCTCCAAGG		
SUV39H1	F	TGGAGAAGATCCGCAAGAAC	ENSCAFG00000015545	Gulay et al., 2021
	R	TGTACACGTCCTCCACGTAGTC		
SUV39H2	F	CGATTGGAATCACCAAAAGG	ENSCAFG00000004696	Gulay et al., 2021
	R	AGAATCTGGCCATCCTTTCC		
MLL1	F	GCTTTGGCTCCAGCAAGAAC	ENSCAFG00000012691	Gulay et al., 2021
	R	CGTCAGTGACTTCCAGGCAT		
MLL3	F	TCGCTCCAAGAAAAGGAAGA	ENSCAFG00000004955	Gulay et al., 2021
	R	CAAGCCATAGGAGGTGGTGT		
DOT1L	F	ACCACGATGCTGCTCATGAA	ENSCAFG00000019420	Gulay et al., 2021
	R	GCCTCTGCATGCTTTCGAAG		
G9A	F	GAAGAAGTGGCGGAAGGACA	ENSCAFG00000000669	Gulay et al., 2021
	R	ACTCACTAGGGCCTGAGGAG		
NSD1	F	TATGGAGGGGGATGTGAGCA	ENSCAFG00000016473	Gulay et al., 2021
	R	GGTCTTCCTGCAGCTGTCTT		
P15INK4B	F	GTGCGGCAGCTCCTGGAAGC	ENSCAFG00000001675	Gulay et al., 2021
	R	GCCCATCATCATGACCTGGATCG		
P16INK4A	F	GTGGACCTGGCTGAGGAGCG	ENSCAFG00040004457	Gulay et al., 2021
	R	TTCTTGAAGTCCGGGCTGTCTG		
ATR	F	CAGCGCTTCCTAGTACTCCG	ENSCAFG00000007863	Gulay et al., 2021
	R	TTGGCAGCAAGGTCAGGTAG		
IF144L	F	TCTATTTTCCGAGGCCAGAG	ENSCAFG00000020343	Gulay et al., 2021
	R	TCATGTATCCCCATGGAGTC		
CD40	F	TATTCACCTCGCCATGGTTC	ENSCAFG00000009994	Gulay et al., 2021
	R	GAGTGCATTCCGTGTCAATG		
CCR7	F	GGCTCTCCTTGTCATTTTCC	ENSCAFG00000030300	

	R	TCCACCGTGGTATTTTCTCC		Gulay et al., 2021
OAS1	F	TGTGCGGGTGTCTAAAGTTG	ENSCAFG00000023556	Gulay et al., 2021
	R	TGAACTGTCCTCGTTTCTCG		
OAS2	F	TGACCCAGATCCAGAAAACC	ENSCAFG00000023107	Gulay et al., 2021
	R	CCATTCGGTAGCGTCTTTTG		
PROCR	F	GCAGGAACACAATGCTTCAA	ENSCAFG00000007945	Aoshima *et al.*, 2018
	R	AAGATGCCTACAGCCACACC		
TNFAIP3	F	GGTGATCGAAATTCCTGTCC	ENSCAFG00000000267	Gulay et al., 2021
	R	TGGGTAAGTTGGCTTCATCC		
BAX	F	ACATGGAGTTGCAGAGGATG	ENSCAFG00000003867	Gulay et al., 2021
	R	CCAGTTGAAGTTGCCATCAG		
RB1	F	AAGCAGAAGCCAACTTGACCAG	ENSCAFG00000004436	Gulay et al., 2021
	R	GTCCTTCTCGGTCTTTTGCTTG		
MCL1	F	AGCTGCATCGAACCATTAGC	ENSCAFG00000012050	Gulay et al., 2021
	R	AGAACTCCACAAACCCATCC		
E2F1	F	GATGGTCATGGTGATCAAGG	ENSCAFG00000007429	Gulay et al., 2021
	R	GCACAGGAAAACGTCAATGG		
CDC25A	F	CCTGAAAAGGAGCCATTCTG	ENSCAFG00000012919	Gulay et al., 2021
	R	ACGGGGTCTCTTCATCATTG		
p18	F	GCTGCAGGTTATGAAACTTGG	ENSCAFG00000028905	Gulay et al., 2021
	R	CGAAACCAGTTCGGTCTTTC		
BRCA2	F	CGGGAGATTGACTGTGGGTC	ENSCAFG00000006383	Gulay et al., 2021
	R	GCAAGCAGGACGAGTACTGT		
HSPA8	F	AACCACCCCAAGTTATGTCG	ENSCAFG00000011666	Gulay et al., 2021
	R	TCAGATTGGACGACAGCATC		
JAK1	F	TACGGACAACATCAGCTTCG	ENSCAFG00000018615	Gulay et al., 2021
	R	TGAGGATCCGGTCAAAACTC		
JAK2	F	TCAGATGTCTGGAGCTTTGG	ENSCAFG00000002102	Gulay et al., 2021
	R	TCATCTGTCCTTGCTTGTCG		

	JAG1	F	GAAGCGTGGGATTCCAGTAA	ENSCAFG00000005627	Gulay et al., 2021
		R	CAGAACTTGTTGCAGCCAAA		
	JAG2	F	AGGGCAGTACCTGCAACATC	ENSCAFG00000018401	Gulay et al., 2021
		R	TGCAGGAGAACGAGTCAATG		
	HEY1	F	GCGCGGATGAGAATGGAAAC	ENSCAFG00000008391	Aoshima *et al.*, 2018
		R	GTCGGCGCTTCTCAATGATG		
	HEY2	F	CGGCGAGATCGGATAAATAA	ENSCAFG00000032212	Aoshima *et al.*, 2018
		R	CGCGTCGAAGTAGCCTTTAC		
	DLL1	F	CCGATGACCTCACAACAGAA	ENSCAFG00000004094	Gulay et al., 2021
		R	GCAGACCTTCTCCCCTCTCT		
	VEGFA	F	TATGGCAGGAGGAGAGCACAAACC	ENSCAFG00000001938	Gulay et al., 2021
		R	CAGCCCCCACACCGCATCAG		
	NOTCH1	F	TACCGGCCAGAACTGTGAGGAGAA	ENSCAFG00000019633	Aoshima *et al.*, 2018
		R	GGAGGGCAGCGGCAGTTGTAAGTA		
	NOCTH2	F	TCGGGATAGCTATGAGCCCT	ENSCAFG00000010476	Aoshima *et al.*, 2018
		R	GGCATGTTGCTTTCCCCAAC		
	FGFR1	F	TCCGTCAATGTCTCAGATGC	ENSCAFG00000005970	Gulay et al., 2021
		R	CCATCTTTTCTGGGGATGTC		
	FGFR2	F	TCCGTCAATGTCTCAGATGC	ENSCAFG00000012374	Gulay et al., 2021
		R	CCATCTTTTCTGGGGATGTC		
	PLOD2	F	TATGGCTCTCTGCCGAAATG	ENSCAFG00000008101	Gulay et al., 2021
		R	TGGAATGTTTCCGGAGTAGG		
	SDC1	F	TCTGGGGATGACTCTGACAAC	ENSCAFG00000003833	Gulay et al., 2021
		R	TCTGCTGTGACAAGGTGATG		
	HSPA5	F	CGGAGGCTTATTTGGGAAAG	ENSCAFG00000020196	Gulay et al., 2021
		R	TGGGCATCATTGAAGTAGGC		
	PDK3	F	TGTCCATCAAGCAGTTCCTG	ENSCAFG00000013476	

		R	AGCAAGTTATCCGGCAGAAG		Gulay et al., 2021
	MYC	F	CGCTGGTCCTTAAGAGATGC	ENSCAFG00000001086	Gulay et al., 2021
		R	CGCCTCTTGTCATTCTCCTC		
Human	*KDM1A*	F	CCCATGGAAACTGGAATAGC	ENSG00000004487	Gulay et al., 2021
		R	GCCAAGCTTTCATCCATCTC		
	KDM2A	F	AAGAAATGTGTCCCCACAGG	ENSG00000173120	Gulay et al., 2021
		R	CAAGCTCCTCCAGCAAAATC		
	KDM2B	F	ATGCCTGACCCTGATTTCAC	ENSG00000089094	Gulay et al., 2021
		R	TGGGTGTTCACATCCATCAC		
	EZH2	F	TTTCCAGATAAGGGCACAGC	ENSG00000106462	Gulay et al., 2021
		R	ATGTTGGGGGTACATTCAGG		
	G9A	F	GGTTTGCGCTTCAACTCAAC	ENSG00000204371	Gulay et al., 2021
		R	AATGGGCACGTTCTCATAGC		
	MLL1	F	TGCCTGGAAGTCATTGACAG	ENSG00000118058	Gulay et al., 2021
		R	GGAACACAACTGCATCATGG		
	SETD6	F	AGGATGAAAAGGAGCCCAAC	ENSG00000103037	Gulay et al., 2021
		R	TTTAGGAATGGGCTGAGTGG		
	SMYD5	F	TGAAGGATCTGGCCTCTTTG	ENSG00000135632	Gulay et al., 2021
		R	AAAGGAGGTCTCTGCATTGG		
	SUV39H2	F	TCGATACGGCAATGTGTCTC	ENSG00000152455	Gulay et al., 2021
		R	CAATGCTATTCGGGGAAGAC		

Table 3. List of shRNA oligos used in the study.

Species	Name	Sequence	Reference
Canine	KDM1A-A	AAGUGAUACUGUGCUAGUCCAC	Gulay et al., 2021
	KDM1A-B	ACUUCAGGAUGUGAAGUGAUAG	Gulay et al., 2021
	KDM1A-C	GUAUAGAGCAAGAGAAGCAGAU	Gulay et al., 2021
	KDM2A-A	AGCUCUCAGUGGCAUCAUCAAG	Gulay et al., 2021
	KDM2A-B	CAUGCUGUAUCUGCAAUGAGAU	Gulay et al., 2021
	KDM2A-C	CGCCCACAACCUGGAGCUGUAC	Gulay et al., 2021
	KDM2B-A	ACCACAGCAUCUGAAGGAGAAG	Gulay et al., 2021
	KDM2B-B	CCCAGUGCCUGUCCUUCUUCAA	Gulay et al., 2021
	KDM2B-C	CCCAGAGAGAAUCCAUGCUUAU	Gulay et al., 2021
	KDM2B-3	UGGAAAUAUCUGUCAUAUUGA	Gulay et al., 2021
	KDM2B-4	CAGUUCAUAGCUGAAAUGUCU	Gulay et al., 2021
	scramble 1	AUAAGAGACGAACGUAACAUA	Gulay et al., 2021
	scramble 5	AGAAGAUUAACGUAGAAGGUG	Gulay et al., 2021

Table 4. List of oligos used for the induction of mutations in KDM2B sequence.

Species	Target	Sequence		Reference
Canine	WT KDM2B	F	CGCTACCGGTCTCGAGACCATGCATCGGGCAGTGGACCCTC	Gulay et al., 2021
		R	CGACGGTACCGAATTCCAGAGGCGGGACCTAGGTCCAGC	
	Silent mutation for shKDM2B C	F	CGCGAGTCTATGCTGATTGATGCCCCAAGAAAGCC	Gulay et al., 2021
		R	CAGCATAGACTCGCGTTGGTATTCCTGAGTGAGGT	
	$KDM2B^{H283Y}$	F	TGGATTTACGCAGTCTACACCCCCGTA	Gulay et al., 2021
		R	GACTGCGTAAATCCAACCGGAAGG	
	$KDM2B^{C587A}$	F	ACGCGAGCCCGCAAGTGCGAGGCC	Gulay et al., 2021
		R	CGCCGGACGCGAGCCCGCAAG	
	$KDM2B^{\triangle PHD}$	F	GCGCCAGTGCTGCCCCATGGCAAGACCGGGAAACAAAA	Gulay et al., 2021
		R	TTTCCCGGTCTTGCCATGGGGCAGCACTGGCGCGA	

Conclusions

I have presented various evidences which demonstrate the role of KDM2B as an oncogene in HSA by regulating DNA repair system and apoptosis. This study provided sufficient evidence that KDM2B can be used as a biomarker to aid differential diagnosis between HSA and HMA. I also demonstrated that a histone demethylase inhibitor GSK-J4 can work as a new therapeutic alternative to doxorubicin treatment in HSA. To the author's knowledge, this is the first epigenetic study in canine HSA. These findings shed light on epigenetic pathology and provide a new insight for novel therapies in HSA. To further understand the role of KDM2B in HSA pathology, future studies should focus on establishing the relationship of the KDM2B expression to several patient profile such as age, sex, breed, effectivity of treatment methods, survival, and treatment outcomes. At present, *in vivo* analysis of canine HSA is limited to the use of an immunocompromised mouse model. This can impede the analysis of the role of immune cells, important factor of tumor microenvironment, in HSA development and progression. Thus, establishing a syngeneic model for canine HSA should also be prioritized.

Summary in Japanese

血管肉腫は血管内皮細胞由来の悪性腫瘍であり，脾臓・肝臓・心右心耳に好発する。どの動物にも起こりうるが，特にイヌでは高頻度に発生し，ヒトではまれである．血管肉腫に対する有効な治療法は存在せず，新規治療法の開発が望まれているものの，その病態の詳細は未だ明らかではない．エピジェネティクスとは DNA 塩基配列の変化を伴わない遺伝子発現制御機構である．DNA とともにクロマチンを構成するヒストンタンパク質は，メチル化やアセチル化などの修飾を受けることによって，クロマチン構造を変化させて遺伝子発現を制御する．がん細胞ではエピジェネティクス異常が生じており，遺伝子発現が正常に制御されていない．このため，エピジェネティクス異常は細胞のがん化にも深く関与していると考えられる．しかし，血管肉腫のエピジェネティクスに関する研究はこれまでに報告がなく，その役割は未だ明らかではない．本研究ではイヌ血管肉腫のエピジェネティクス機構に着目し，エピジェネティクスが血管肉腫の病態に果たす役割を明らかにすることを目的とした．

まず筆者はイヌ正常血管内皮細胞とイヌ血管肉腫細胞におけるエピジェネティクス関連遺伝子の発現を調べ，ヒストン脱メチル化酵素 KDM2B が血管肉腫細胞で高発現していることを明らかにした． 次に，血管肉腫細胞において KDM2B をノックダウンすると，細胞死が誘導されることがわかった．KDM2B ノックダウン血管肉腫細胞では DNA 修復機構の活性が抑制されており，その結果 DNA ダメージが蓄積することによって，アポトーシスが誘導されていることがわかった．次に，イヌ血管肉腫細胞をヌードマウスに移植し，腫瘍が形成されてから KDM2B をノックダウンしたところ，腫瘍の退縮が認められ，KDM2B は in vivo でも腫瘍細胞の生存・増殖に必須であることがわかった．また，臨床症例を用いた解析でも KDM2B は血管肉腫細胞で高発現しており，臨床例においても KDM2B が重要な役割を有していることが示唆された．さらに新規治療法の可能性を探るため，ヒストン脱メチル化酵素の阻害剤である GSK-J4 が血管肉腫に対して効果を示すかどうかを調べた．その結果，GSK-J4 は KDM2B ノックダウンと同様の機構で細胞死を誘導し，in vivo においても腫瘍の増殖を遅らせることが明らかになった．これらの結果から，GSK-J4 はイヌ血管肉腫におけるドキソルビシン治療に代わる新たな治療法として機能しうることがわかった．

筆者の知る限り，本研究はイヌ血管肉腫における初めてのエピジェネティクス研究であり，これらの結果は血管肉腫に対する新規治療法開発への基礎となるもの

である．血管肉腫の病態における KDM2B の役割をさらに理解するために，今後の研究では，イヌの年齢，性別，品種，治療法の効果，生存率，治療成績などの患者プロファイルと KDM2B との関係を明らかにすることが重要である．また，現段階では，血管肉腫の in vivo 解析を行うためには免疫不全マウスを使用なくてはならない．しかし，免疫細胞は腫瘍微小環境の重要な一要素であり，真の血管肉腫の病態を明らかにすることはできない．したがって、血管肉腫のための同種移植モデル (syngeneic model) を確立する必要がある。

Acknowledgements

Firstly, I am greatly indebted to my professor, Dr. Takashi Kimura (Laboratory of Comparative Pathology, Hokkaido University) for his willingness to accept me as a PhD student in his laboratory and for his guidance and support during the course of my study.

I would also like to thank Dr. Atsushi Kobayashi (Laboratory of Comparative Pathology, Hokkaido University) for his guidance and for giving me opportunities to learn and grow as a researcher.

I am also thankful for Dr. Keisuke Aoshima (Laboratory of Comparative Pathology, Hokkaido University) for teaching me everything I know about cancer epigenetics, pathology, and molecular biology. Without his patience and guidance, I would not be the person and researcher that I am today.

I would also like to express my gratitude to all my co-authors in all my publication: Dr. Yuki Shibata (Laboratory of Radiation Biology, Hokkaido University), Dr. Hironobu Yasui (Laboratory of Radiation Biology, Hokkaido University), and Dr. Qin Yan (Department of Pathology, Yale University) for their major contribution to the development of my studies. This thesis would not be possible without the guidance from my advisers: Dr. Noboru Sasaki (Laboratory of Internal Medicine, Hokkaido University), Dr. Jumpei Yamazaki (Veterinary Teaching Hospital, Hokkaido University), and Dr. Osamu Ichii (Laboratory of Anatomy, Hokkaido University). I would also like to thank the head of my thesis committee: Dr. Mitsuyoshi Takiguchi (Veterinary Teaching Hospital, Hokkaido University) for his time and for his invaluable insights which helped improve the significance of this study.

I would also like to express my heartfelt gratitude to the former and present members of the Laboratory of Comparative Pathology, Hokkaido University for their invaluable assistance and support.

I would like to acknowledge the support of the Ministry of Education, Science and Culture of Iceland on Education, Science, Technology and Innovation (MEXT) and the Japan Science Society (JSS) for providing me with the means to conduct and perform my studies here in Hokkaido University.

I am also thankful to all the former and present members of Hokkaido

Association of Filipino Students (HAFS) who made me feel at home here in Hokkaido, Japan and for all the memories the good moments we have shared. I would also like to extend my sincerest gratitude to my seniors, Dr. Yuki Otani (Laboratory of Anatomy, Hokkaido University), Dr. Masahiro Tamura (Laboratory of Internal Medicine, Hokkaido University), and Dr. Emmanuel Hernandez (Kagoshima University) for their kindness and generosity and for always being there whenever I needed support and help.

I would always be indebted to Dr. Ignacia Tanaka and Dr. Satoshi Tanaka for giving me a chance to improve myself, for serving as my mentors, and for giving me an opportunity to pursue graduate studies in Hokkaido University. Words are not enough to express how grateful I am to these people.

I would like to acknowledge my family, especially siblings, Angel and Lance for their encouragement, love, and for making sure that I always stay grounded. Finally, I would like to dedicate this thesis to my mother, Cecilia Montecillo Gulay, I hope I made you proud.

References

1. Adjiri, A. (2016). Identifying and Targeting the Cause of Cancer is Needed to Cure Cancer. *Oncology and Therapy*, *4*(1), 17–33. https://doi.org/10.1007/s40487-015-0015-6
2. Aoshima, K., Fukui, Y., Gulay, K. C. M., Erdemsurakh, O., Morita, A., Kobayashi, A., & Kimura, T. (2018). Notch2 signal is required for the maintenance of canine hemangiosarcoma cancer stem cell-like cells. *BMC Veterinary Research*, *14*(1), 301. https://doi.org/10.1186/s12917-018-1624-8
3. Arruebo, M., Vilaboa, N., Sáez-Gutierrez, B., Lambea, J., Tres, A., Valladares, M., & González-Fernández, Á. (2011). Assessment of the Evolution of Cancer Treatment Therapies. *Cancers*, *3*(3), 3279–3330. https://doi.org/10.3390/cancers3033279
4. Bankhead, P., Loughrey, M. B., Fernández, J. A., Dombrowski, Y., McArt, D. G., Dunne, P. D., McQuaid, S., Gray, R. T., Murray, L. J., Coleman, H. G., James, J. A., Salto-Tellez, M., & Hamilton, P. W. (2017). QuPath: Open source software for digital pathology image analysis. *Scientific Reports*, *7*(1), 16878. https://doi.org/10.1038/s41598-017-17204-5
5. Batschinski, K., Nobre, A., Vargas-Mendez, E., Tedardi, M. V., Cirillo, J., Cestari, G., Ubukata, R., & Dagli, M. L. Z. (2018). Canine visceral hemangiosarcoma treated with surgery alone or surgery and doxorubicin: 37 cases (2005-2014). *The Canadian Veterinary Journal = La Revue Veterinaire Canadienne*, *59*(9), 967–972.
6. Boom, V. van den, Maat, H., Geugien, M., López, A. R., Sotoca, A. M., Jaques, J., Brouwers-Vos, A. Z., Fusetti, F., Groen, R. W. J., Yuan, H., Martens, A. C. M., Stunnenberg, H. G., Vellenga, E., Martens, J. H. A., & Schuringa, J. J. (2016). Non-canonical PRC1.1 Targets Active Genes Independent of H3K27me3 and Is Essential for Leukemogenesis. *Cell Reports*, *14*(2), 332–346. https://doi.org/10.1016/j.celrep.2015.12.034
7. Brzostek-Racine, S., Gordon, C., Scoy, S. V., & Reich, N. C. (2011). The DNA Damage Response Induces IFN. *The Journal of Immunology*, *187*(10), 5336–5345. https://doi.org/10.4049/jimmunol.1100040
8. Carvalho, C., Santos, R., Cardoso, S., Correia, S., Oliveira, P., Santos, M., & Moreira, P. (2009). Doxorubicin: The Good, the Bad and the Ugly Effect. *Current*

Medicinal Chemistry, *16*(25), 3267–3285. https://doi.org/10.2174/092986709788803312

9. Chen, J., Harding, S. M., Natesan, R., Tian, L., Benci, J. L., Li, W., Minn, A. J., Asangani, I. A., & Greenberg, R. A. (2020). Cell Cycle Checkpoints Cooperate to Suppress DNA- and RNA-Associated Molecular Pattern Recognition and Anti-Tumor Immune Responses. *Cell Reports*, *32*(9), Article 9. https://doi.org/10.1016/j.celrep.2020.108080
10. Chen, L., Fu, L., Kong, X., Xu, J., Wang, Z., Ma, X., Akiyama, Y., Chen, Y., & Fang, J. (2014). Jumonji domain-containing protein 2B silencing induces DNA damage response via STAT3 pathway in colorectal cancer. *British Journal of Cancer*, *110*(4), 1014–1026. https://doi.org/10.1038/bjc.2013.808
11. Clifford, C. A., Mackin, A. J., & Henry, C. J. (2000). Treatment of Canine Hemangiosarcoma: 2000 and Beyond. *Journal of Veterinary Internal Medicine*, *14*(5), 479–485. https://doi.org/10.1111/j.1939-1676.2000.tb02262.x
12. Dawson, M. A., & Kouzarides, T. (2012). Cancer Epigenetics: From Mechanism to Therapy. *Cell*, *150*(1), 12–27. https://doi.org/10.1016/j.cell.2012.06.013
13. Dobin, A., Davis, C. A., Schlesinger, F., Drenkow, J., Zaleski, C., Jha, S., Batut, P., Chaisson, M., & Gingeras, T. R. (2013). STAR: Ultrafast universal RNA-seq aligner. *Bioinformatics*, *29*(1), 15–21. https://doi.org/10.1093/bioinformatics/bts635
14. Edelheit, O., Hanukoglu, A., & Hanukoglu, I. (2009). Simple and efficient site-directed mutagenesis using two single-primer reactions in parallel to generate mutants for protein structure-function studies. *BMC Biotechnology*, *9*(1), 61. https://doi.org/10.1186/1472-6750-9-61
15. Fosmire, S. P., Dickerson, E. B., Scott, A. M., Bianco, S. R., Pettengill, M. J., Meylemans, H., Padilla, M., Frazer-Abel, A. A., Akhtar, N., Getzy, D. M., Wojcieszyn, J., Breen, M., Helfand, S. C., & Modiano, J. F. (2004). Canine malignant hemangiosarcoma as a model of primitive angiogenic endothelium. *Laboratory Investigation*, *84*(5), 562–572. https://doi.org/10.1038/labinvest.3700080
16. Goodman, L. S., & Wintrobe, M. M. (1946). Nitrogen mustard therapy; use of methyl-bis (beta-chloroethyl) amine hydrochloride and tris (beta-chloroethyl) amine hydrochloride for Hodgkin's disease, lymphosarcoma, leukemia and certain allied and miscellaneous disorders. *Journal of the American Medical Association*, *132*,

126–132. https://doi.org/10.1001/jama.1946.02870380008004

17. Guzmán, C., Bagga, M., Kaur, A., Westermarck, J., & Abankwa, D. (2014). ColonyArea: An ImageJ Plugin to Automatically Quantify Colony Formation in Clonogenic Assays. *PLOS ONE*, *9*(3), e92444. https://doi.org/10.1371/journal.pone.0092444
18. Han, X.-R., Zha, Z., Yuan, H.-X., Feng, X., Xia, Y.-K., Lei, Q.-Y., Guan, K.-L., & Xiong, Y. (2016). KDM2B/FBXL10 targets c-Fos for ubiquitylation and degradation in response to mitogenic stimulation. *Oncogene*, *35*(32), 4179–4190. https://doi.org/10.1038/onc.2015.482
19. Harasawa, R., Mizusawa, H., Nozawa, K., Nakagawa, T., Asada, K., & Kato, I. (1993). Detection and tentative identification of dominant mycoplasma species in cell cultures by restriction analysis of the 16S-23S rRNA intergenic spacer regions. *Research in Microbiology*, *144*(6), 489–493. https://doi.org/10.1016/0923-2508(93)90057-9
20. Harasawa, Ryô, Mizusawa, H., Fujii, M., Yamamoto, J., Mukai, H., Uemori, T., Asada, K., & Kato, I. (2005). Rapid detection and differentiation of the major mycoplasma contaminants in cell cultures using real-time PCR with SYBR Green I and melting curve analysis. *Microbiology and Immunology*, *49*(9), 859–863. https://doi.org/10.1111/j.1348-0421.2005.tb03675.x
21. He, J., Nguyen, A. T., & Zhang, Y. (2011). KDM2B/JHDM1b, an H3K36me2-specific demethylase, is required for initiation and maintenance of acute myeloid leukemia. *Blood*, *117*(14), 3869–3880. https://doi.org/10.1182/blood-2010-10-312736
22. Heidelberger, C., Chaudhuri, N. K., Danneberg, P., Mooren, D., Griesbach, L., Duschinsky, R., Schnitzer, R. J., Pleven, E., & Scheiner, J. (1957). Fluorinated pyrimidines, a new class of tumour-inhibitory compounds. *Nature*, *179*(4561), 663–666. https://doi.org/10.1038/179663a0
23. Heinemann, B., Nielsen, J. M., Hudlebusch, H. R., Lees, M. J., Larsen, D. V., Boesen, T., Labelle, M., Gerlach, L.-O., Birk, P., & Helin, K. (2014). Inhibition of demethylases by GSK-J1/J4. *Nature*, *514*(7520), E1–E2. https://doi.org/10.1038/nature13688
24. Hong, X., Xu, Y., Qiu, X., Zhu, Y., Feng, X., Ding, Z., Zhang, S., Zhong, L., Zhuang, Y., Su, C., Hong, X., & Cai, J. (2016). MiR-448 promotes glycolytic metabolism of

gastric cancer by downregulating KDM2B. *Oncotarget*, *7*(16), 22092–22102. https://doi.org/10.18632/oncotarget.8020

25. Huang, L., Snyder, A. R., & Morgan, W. F. (2003). Radiation-induced genomic instability and its implications for radiation carcinogenesis. *Oncogene*, *22*(37), 5848–5854. https://doi.org/10.1038/sj.onc.1206697
26. Johannes, C. M., Henry, C. J., Turnquist, S. E., Hamilton, T. A., Smith, A. N., Chun, R., & Tyler, J. W. (2007). Hemangiosarcoma in cats: 53 cases (1992-2002). *Journal of the American Veterinary Medical Association*, *231*(12), 1851–1856. https://doi.org/10.2460/javma.231.12.1851
27. Kim, J. J., & Tannock, I. F. (2005). Repopulation of cancer cells during therapy: An important cause of treatment failure. *Nature Reviews. Cancer*, *5*(7), 516–525. https://doi.org/10.1038/nrc1650
28. Kim, J.-H., Graef, A. J., Dickerson, E. B., & Modiano, J. F. (2015). Pathobiology of Hemangiosarcoma in Dogs: Research Advances and Future Perspectives. *Veterinary Sciences*, *2*(4), 388–405. https://doi.org/10.3390/vetsci2040388
29. Kottakis, F., Foltopoulou, P., Sanidas, I., Keller, P., Wronski, A., Dake, B. T., Ezell, S. A., Shen, Z., Naber, S. P., Hinds, P. W., McNiel, E., Kuperwasser, C., & Tsichlis, P. N. (2014). NDY1/KDM2B functions as a master regulator of polycomb complexes and controls self-renewal of breast cancer stem cells. *Cancer Research*, *74*(14), 3935–3946. https://doi.org/10.1158/0008-5472.CAN-13-2733
30. Kottakis, F., Polytarchou, C., Foltopoulou, P., Sanidas, I., Kampranis, S. C., & Tsichlis, P. N. (2011). FGF-2 regulates cell proliferation, migration, and angiogenesis through an NDY1/KDM2B-miR-101-EZH2 pathway. *Molecular Cell*, *43*(2), 285–298. https://doi.org/10.1016/j.molcel.2011.06.020
31. Kurt, I. C., Sur, I., Kaya, E., Cingoz, A., Kazancioglu, S., Kahya, Z., Toparlak, O. D., Senbabaoglu, F., Kaya, Z., Ozyerli, E., Karahüseyinoglu, S., Lack, N. A., Gümüs, Z. H., Onder, T. T., & Bagci-Onder, T. (2017). KDM2B, an H3K36-specific demethylase, regulates apoptotic response of GBM cells to TRAIL. *Cell Death & Disease*, *8*(6), e2897. https://doi.org/10.1038/cddis.2017.288
32. Li, B., & Dewey, C. N. (2011). RSEM: Accurate transcript quantification from RNA-Seq data with or without a reference genome. *BMC Bioinformatics*, *12*(1), 323. https://doi.org/10.1186/1471-2105-12-323

33. Li, Y., Zhang, M., Sheng, M., Zhang, P., Chen, Z., Xing, W., Bai, J., Cheng, T., Yang, F.-C., & Zhou, Y. (2018). Therapeutic potential of GSK-J4, a histone demethylase KDM6B/JMJD3 inhibitor, for acute myeloid leukemia. *Journal of Cancer Research and Clinical Oncology*, *144*(6), 1065–1077. https://doi.org/10.1007/s00432-018-2631-7
34. Maharani, A., Aoshima, K., Onishi, S., Gulay, K. C. M., Kobayashi, A., & Kimura, T. (2018). Cellular atypia is negatively correlated with immunohistochemical reactivity of CD31 and vWF expression levels in canine hemangiosarcoma. *Journal of Veterinary Medical Science*, *80*(2), 213–218. https://doi.org/10.1292/jvms.17-0561
35. Mboko, W. P., Mounce, B. C., Wood, B. M., Kulinski, J. M., Corbett, J. A., & Tarakanova, V. L. (2012). Coordinate Regulation of DNA Damage and Type I Interferon Responses Imposes an Antiviral State That Attenuates Mouse Gammaherpesvirus Type 68 Replication in Primary Macrophages. *Journal of Virology*, *86*(12), 6899–6912. https://doi.org/10.1128/JVI.07119-11
36. Meerbrey, K. L., Hu, G., Kessler, J. D., Roarty, K., Li, M. Z., Fang, J. E., Herschkowitz, J. I., Burrows, A. E., Ciccia, A., Sun, T., Schmitt, E. M., Bernardi, R. J., Fu, X., Bland, C. S., Cooper, T. A., Schiff, R., Rosen, J. M., Westbrook, T. F., & Elledge, S. J. (2011). The pINDUCER lentiviral toolkit for inducible RNA interference *in vitro* and *in vivo*. *Proceedings of the National Academy of Sciences of the United States of America*, *108*(9), 3665–3670. https://doi.org/10.1073/pnas.1019736108
37. Megquier, K., Turner-Maier, J., Swofford, R., Kim, J.-H., Sarver, A. L., Wang, C., Sakthikumar, S., Johnson, J., Koltookian, M., Lewellen, M., Scott, M. C., Schulte, A. J., Borst, L., Tonomura, N., Alfoldi, J., Painter, C., Thomas, R., Karlsson, E. K., Breen, M., … Lindblad-Toh, K. (2019). Comparative Genomics Reveals Shared Mutational Landscape in Canine Hemangiosarcoma and Human Angiosarcoma. *Molecular Cancer Research*, *17*(12), 2410–2421. https://doi.org/10.1158/1541-7786.MCR-19-0221
38. Moffat, J., Grueneberg, D. A., Yang, X., Kim, S. Y., Kloepfer, A. M., Hinkle, G., Piqani, B., Eisenhaure, T. M., Luo, B., Grenier, J. K., Carpenter, A. E., Foo, S. Y., Stewart, S. A., Stockwell, B. R., Hacohen, N., Hahn, W. C., Lander, E. S., Sabatini, D. M., & Root, D. E. (2006). A Lentiviral RNAi Library for Human and Mouse Genes Applied to an Arrayed Viral High-Content Screen. *Cell*, *124*(6), 1283–1298.

https://doi.org/10.1016/j.cell.2006.01.040

39. Moosavi, A., & Motevalizadeh Ardekani, A. (2016). Role of Epigenetics in Biology and Human Diseases. *Iranian Biomedical Journal*, *20*(5), 246–258. https://doi.org/10.22045/ibj.2016.01
40. Mootha, V. K., Lindgren, C. M., Eriksson, K.-F., Subramanian, A., Sihag, S., Lehar, J., Puigserver, P., Carlsson, E., Ridderstråle, M., Laurila, E., Houstis, N., Daly, M. J., Patterson, N., Mesirov, J. P., Golub, T. R., Tamayo, P., Spiegelman, B., Lander, E. S., Hirschhorn, J. N., … Groop, L. C. (2003). PGC-1alpha-responsive genes involved in oxidative phosphorylation are coordinately downregulated in human diabetes. *Nature Genetics*, *34*(3), 267–273. https://doi.org/10.1038/ng1180
41. Morin, R. D., Mendez-Lago, M., Mungall, A. J., Goya, R., Mungall, K. L., Corbett, R. D., Johnson, N. A., Severson, T. M., Chiu, R., Field, M., Jackman, S., Krzywinski, M., Scott, D. W., Trinh, D. L., Tamura-Wells, J., Li, S., Firme, M. R., Rogic, S., Griffith, M., … Marra, M. A. (2011). Frequent mutation of histone-modifying genes in non-Hodgkin lymphoma. *Nature*, *476*(7360), 298–303. https://doi.org/10.1038/nature10351
42. Morita, A., Aoshima, K., Gulay, K. C. M., Onishi, S., Shibata, Y., Yasui, H., Kobayashi, A., & Kimura, T. (2019). High drug efflux pump capacity and low DNA damage response induce doxorubicin resistance in canine hemangiosarcoma cell lines. *Research in Veterinary Science*, *127*, 1–10. https://doi.org/10.1016/j.rvsc.2019.09.011
43. Murai, A., Asa, S. A., Kodama, A., Hirata, A., Yanai, T., & Sakai, H. (2012). Constitutive phosphorylation of the mTORC2/Akt/4E-BP1 pathway in newly derived canine hemangiosarcoma cell lines. *BMC Veterinary Research*, *8*(1), 128. https://doi.org/10.1186/1746-6148-8-128
44. Odom, A. L., Hatwig, C. A., Stanley, J. S., & Benson, A. M. (1992). Biochemical determinants of adriamycin® toxicity in mouse liver, heart and intestine. *Biochemical Pharmacology*, *43*(4), 831–836. https://doi.org/10.1016/0006-2952(92)90250-M
45. Peta, E., Sinigaglia, A., Masi, G., Di Camillo, B., Grassi, A., Trevisan, M., Messa, L., Loregian, A., Manfrin, E., Brunelli, M., Martignoni, G., Palù, G., & Barzon, L. (2018). HPV16 E6 and E7 upregulate the histone lysine demethylase KDM2B through the

c-MYC/miR-146a-5p axys. *Oncogene*, *37*(12), 1654–1668. https://doi.org/10.1038/s41388-017-0083-1

46. Peters, I. R., Peeters, D., Helps, C. R., & Day, M. J. (2007). Development and application of multiple internal reference (housekeeper) gene assays for accurate normalisation of canine gene expression studies. *Veterinary Immunology and Immunopathology*, *117*(1–2), 55–66. https://doi.org/10.1016/j.vetimm.2007.01.011
47. Prymak, C., McKee, L. J., Goldschmidt, M. H., & Glickman, L. T. (1988). Epidemiologic, clinical, pathologic, and prognostic characteristics of splenic hemangiosarcoma and splenic hematoma in dogs: 217 cases (1985). *Journal of the American Veterinary Medical Association*, *193*(6), 706–712.
48. Robinson, M. D., McCarthy, D. J., & Smyth, G. K. (2010). edgeR: A Bioconductor package for differential expression analysis of digital gene expression data. *Bioinformatics*, *26*(1), 139–140. https://doi.org/10.1093/bioinformatics/btp616
49. Sastry, G. A. (1951). Angiosarcoma (hemangioendothelioma) in the thorax of a mule. *The Veterinary Record*, *63*(8), 145–147. https://doi.org/10.1136/vr.63.8.145
50. Schneider, C. A., Rasband, W. S., & Eliceiri, K. W. (2012). NIH Image to ImageJ: 25 years of image analysis. *Nature Methods*, *9*(7), 671–675. https://doi.org/10.1038/nmeth.2089
51. Sharma, S., Kelly, T. K., & Jones, P. A. (2010). Epigenetics in cancer. *Carcinogenesis*, *31*(1), 27–36. https://doi.org/10.1093/carcin/bgp220
52. Sheltzer, J. M., Blank, H. M., Pfau, S. J., Tange, Y., George, B. M., Humpton, T. J., Brito, I. L., Hiraoka, Y., Niwa, O., & Amon, A. (2011). Aneuploidy Drives Genomic Instability in Yeast. *Science*, *333*(6045), 1026–1030. https://doi.org/10.1126/science.1206412
53. Shimizu, H., Nagel, D., & Toth, B. (1974). Ethylhydrazine hydrochloride as a tumor inducer in mice. *International Journal of Cancer*, *13*(4), 500–505. https://doi.org/10.1002/ijc.2910130409
54. Stokes, M. P., Rush, J., Macneill, J., Ren, J. M., Sprott, K., Nardone, J., Yang, V., Beausoleil, S. A., Gygi, S. P., Livingstone, M., Zhang, H., Polakiewicz, R. D., & Comb, M. J. (2007). Profiling of UV-induced ATM/ATR signaling pathways. *Proceedings of the National Academy of Sciences of the United States of America*, *104*(50), 19855–19860. https://doi.org/10.1073/pnas.0707579104

55. Subramanian, A., Tamayo, P., Mootha, V. K., Mukherjee, S., Ebert, B. L., Gillette, M. A., Paulovich, A., Pomeroy, S. L., Golub, T. R., Lander, E. S., & Mesirov, J. P. (2005). Gene set enrichment analysis: A knowledge-based approach for interpreting genome-wide expression profiles. *Proceedings of the National Academy of Sciences*, *102*(43), 15545–15550. https://doi.org/10.1073/pnas.0506580102
56. Thomas, R., Borst, L., Rotroff, D., Motsinger-Reif, A., Lindblad-Toh, K., Modiano, J. F., & Breen, M. (2014). Genomic profiling reveals extensive heterogeneity in somatic DNA copy number aberrations of canine hemangiosarcoma. *Chromosome Research : An International Journal on the Molecular, Supramolecular and Evolutionary Aspects of Chromosome Biology*, *22*(3), 305–319. https://doi.org/10.1007/s10577-014-9406-z
57. Tzatsos, A., Pfau, R., Kampranis, S. C., & Tsichlis, P. N. (2009). Ndy1/KDM2B immortalizes mouse embryonic fibroblasts by repressing the Ink4a/Arf locus. *Proceedings of the National Academy of Sciences*, *106*(8), 2641–2646. https://doi.org/10.1073/pnas.0813139106
58. van Haaften, G., Dalgliesh, G. L., Davies, H., Chen, L., Bignell, G., Greenman, C., Edkins, S., Hardy, C., O'Meara, S., Teague, J., Butler, A., Hinton, J., Latimer, C., Andrews, J., Barthorpe, S., Beare, D., Buck, G., Campbell, P. J., Cole, J., … Futreal, P. A. (2009). Somatic mutations of the histone H3K27 demethylase gene UTX in human cancer. *Nature Genetics*, *41*(5), 521–523. https://doi.org/10.1038/ng.349
59. Wang, T., Chen, K., Zeng, X., Yang, J., Wu, Y., Shi, X., Qin, B., Zeng, L., Esteban, M. A., Pan, G., & Pei, D. (2011). The Histone Demethylases Jhdm1a/1b Enhance Somatic Cell Reprogramming in a Vitamin-C-Dependent Manner. *Cell Stem Cell*, *9*(6), 575–587. https://doi.org/10.1016/j.stem.2011.10.005
60. Wild-Bode, C., Weller, M., Rimner, A., Dichgans, J., & Wick, W. (2001). Sublethal irradiation promotes migration and invasiveness of glioma cells: Implications for radiotherapy of human glioblastoma. *Cancer Research*, *61*(6), 2744–2750.
61. YAMAMOTO, S., HOSHI, K., HIRAKAWA, A., CHIMURA, S., KOBAYASHI, M., & MACHIDA, N. (2013). Epidemiological, Clinical and Pathological Features of Primary Cardiac Hemangiosarcoma in Dogs: A Review of 51 Cases. *The Journal of Veterinary Medical Science*, *75*(11), 1433–1441. https://doi.org/10.1292/jvms.13-0064

62. Yan, M., Yang, X., Wang, H., & Shao, Q. (2018a). The critical role of histone lysine demethylase KDM2B in cancer. *American Journal of Translational Research*, *10*(8), 2222–2233.
63. Yan, M., Yang, X., Wang, H., & Shao, Q. (2018b). The critical role of histone lysine demethylase KDM2B in cancer. *American Journal of Translational Research*, *10*(8), 2222–2233.
64. Yoshino, H., Ueda, T., Kawahata, M., Kobayashi, K., Ebihara, Y., Manabe, A., Tanaka, R., Ito, M., Asano, S., Nakahata, T., & Tsuji, K. (2000). Natural killer cell depletion by anti-asialo GM1 antiserum treatment enhances human hematopoietic stem cell engraftment in NOD/Shi- scid mice. *Bone Marrow Transplantation*, *26*(11), 1211–1216. https://doi.org/10.1038/sj.bmt.1702702
65. Young, R. J., Brown, N. J., Reed, M. W., Hughes, D., & Woll, P. J. (2010). Angiosarcoma. *The Lancet. Oncology*, *11*(10), 983–991. https://doi.org/10.1016/S1470-2045(10)70023-1
66. Zhu, J., Tsai, H.-J., Gordon, M. R., & Li, R. (2018). Cellular Stress Associated with Aneuploidy. *Developmental Cell*, *44*(4), 420–431. https://doi.org/10.1016/j.devcel.2018.02.002